An aerosol-cloud module for inclusion in the KNMI regional climate model RACMO2

Gabriella De Martino, Bert van Ulft,
Harry ten Brink, Martijn Schaap,
Erik van Meijgaard and Reinout Boers

Authors: De Martino, G.
         Ulft, B. van
         Brink, H. ten
         Schaap, M.
         Meijgaard, E. van
         Boers, R.

climate changes spatial planning

● ● ● ●

An aerosol-cloud module for inclusion in the KNMI regional climate model RACMO2

Gabriella De Martino[1], Bert van Ulft[1], Harry ten Brink[2], Martijn Schaap[3], Erik van Meijgaard[1], Reinout Boers[1]

[1] Royal Netherlands Meteorological Institute (KNMI), PO Box 201, 3730 AE De Bilt, The Netherlands
[2] Energy Research Centre of the Netherlands (ECN), PO Box 1, 1755 ZG Petten, The Netherlands
[3] Netherlands Organisation for Applied Scientific research (TNO), Dept. of Air Quality and Climate, P.O.Box 80015, 3508 TA Utrecht, The Netherlands

● ● ● ●

November 2008

Contents

Abstract

This report describes the development and testing of a cloud condensation nuclei (CCN) parameterization in the KNMI regional climate model RACMO2. This requires the parameterization of the cloud droplet number concentration (CDNC) as a function of aerosol loading to allow the computation of the so called indirect aerosol radiative forcing effect. Four CDNC parameterizations were selected and implemented into the Single Column version (SCM) of RACMO2.

The evaluation of the CDNC schemes and their effect on the radiative transfer of clouds has been performed with a set of comprehensive observations made at Cabauw on 30 January 2007. Sensitivity runs with the radiation module of the SCM forced with observations of the atmospheric column at Cabauw show that the internal degrees of freedom of the radiation module overshadow the differences in radiation output arising from the use of different CDNC parameterizations. Moreover, Integrated Profiling Technique retrievals of liquid water path (LWP) available for the testing day were found unrealistically low and required an enhancement factor before being used as input values to the SCM.

At this stage of the investigation we tend to recommend, based on the limited amount of evidence, but also on its potential, the parameterization by Menon et al., (2002) as the most appropriate aerosol/cloud module for application in future studies with RACMO2 of the cloud albedo effect over Europe, in order to assess differences in radiative forcing between pre-industrial and today or future conditions.

Introduction

The main objective of this research is to implement and test a new cloud condensation nuclei (CCN) parameterization in the KNMI regional climate model RACMO2. This parameterization is specifically meant to study the climate impact of the first aerosol indirect effect. The aerosol indirect effect (currently known as Aerosol Cloud Interaction effect) is the modification of cloud microphysics by the presence of extra manmade aerosol particles that serve as extra cloud nuclei and thus affect the radiation transfer of solar radiation of the clouds. As pointed out in the recent IPCC-report AR4, this effect is also known as the cloud albedo effect. In the adopted approach the increased numbers of CCN and resulting cloud droplet numbers are translated into a change of the cloud droplet effective radius R_{eff}, which acts as the key parameter in the model in linking clouds with solar radiation. The report describes the approach to come to this parameterization via a sequence of steps starting with a literature overview of the way to parameterize the transition of aerosols into CCN. The reason is that only part of the total aerosol particles can serve as such. In the approach followed here, aerosol-fields are calculated on the basis of chemical components. Hence a simple parameterization that relates mass concentrations to CCN number concentrations is required for this study.

An overview of existing parameterizations that account for the transition of aerosol into cloud condensation nuclei (CCN) is presented in Chapter 1, where different parameterizations are introduced and a few of them are analyzed in more details. Chapter 2 presents some bibliographical notes about the importance of nitrate as constituents of CCN. Reasons for the choice of four parameterizations that will be used in all following tests are given in Chapter 3, where a study of the sensitivity of cloud albedo to differences in CCN parameterization is reported. In the same chapter, the 3-D chemistry-transport regional model LOTOS-EUROS is introduced. Chapter 4 contains the computations of the maximum possible differences in albedo between pairs of CCN parameterizations and presents the area (Europe) average of the maximum difference in irradiance for one complete year. Chapter 5 provides an overview of all evaluation runs that have been performed in order to test the implementation of the new scheme for the computation of the effective radius in the SCM. Processes involving the onset of precipitation are also known to be affected by aerosols. This is another type of the aerosol indirect effect. To start addressing this topic, a bibliographic overview of autoconversion schemes has been carried out, a summary of which is reported in Chapter 6. Finally, a short discussion of the findings and conclusive remarks are given in Chapter 7. The Appendix describes the actual insertion of the four chosen parameterizations into the climate model.

1   Overview of articles on the parameterization of aerosol into CCN

As an initial task, a bibliographic search of available CCN parameterizations, specifically designed to be used in climate models has been performed. In general, the available CCN parameterizations can be divided into two groups, one based on the aerosol(s) as number of particles per cubic meter or centimeter, or given as mass per volume (micrograms per cubic meters) and transformed into N_d with a lognormal relationship; the second group uses a single mode or multiple mode lognormal size distribution of aerosol, without an explicit distinction among different types of aerosol. There is a third, small group, derived directly from Twomey's (1959) relationship, which relates aerosol number to cloud condensation nuclei via a power law dependence of number as a function of size.
The following list is an overview of parameterizations of the droplet number concentration N_d, with a few comments about the formulation, the origin of data and their range of validity (if applicable). The search has been performed looking in the following sources:

- Work in TAR (3rd IPCC Report, 2001), extended to 2005.
- Bibliographies of authors mentioned in the PhD thesis by Mtinkheni Gondwe, (2004)
- MGA CD from the KNMI Library (only available up to 2002!)
- Internet search using different key words
- Works presented at the "IGAC Specialty Conference on the Indirect Effects of Aerosols on the Global Climate", (2005).

The list reports the formulas for the different parameterizations as they are given in the original papers.

- Raga and Jonas, (1993)

$$N_d = 14 N_a^{0.26}$$

Where N_a is the sub-cloud aerosol number concentration, given in cm^{-3} (and it is valid for values <4000 cm^{-3})

- Jones et al., (1994)

Number of droplets formed on those aerosols that act as CCN, N_{tot}
Concentration of aerosol, A, (cm^{-3})

$$N_{tot} = 375\left(1 - \exp\left[-2.5 \times 10^{-3} A\right]\right)$$

This formula is based on aircraft data by Martin et al. (1994) from a wide range of locations. The formula by Martin et al. (1994) is of the same type.

- Hegg, (1994)

He derives four different linear CCN-Sulphate regression equations for each of the four datasets he takes in consideration and a 'total' one. Together with the formula by Boucher and

Lohmann (1995), his considerations are used in the Hadley Centre GCM model used by Jones and Slingo (1996).

- Boucher and Lohmann, (1995)

They come up with a set of formulations, all based on fitting of data from experimental studies, where sulfate is used as surrogate for all aerosols, assuming that fraction of sulfate that condenses on aerosols remains constant. Each relationship is valid for a specific condition, like continental stratus, continental cumulus or marine clouds. These expressions are used in the ECHAM4 model, and have been quite successful, being used by Lohmann and Feicher (1997), Feicher et al. (1997), Le Treut et al. (1995), Le Treut et al. (1999).
In Boucher and Lohmann (1995) there is especially a relationship, named D, which fits all the dataset:

$$CDNC = 10^{2.21 + 0.41 \log\left[m_{SO_4}\right]}$$

Similar relationships with different constants are given by other authors [Hegg et al. (1993), Novakov and Penner (1993), Novakov et al. (1994)], but they are valid on specific locations, like maritime air mass in Puerto Rico, or SE of the US, or NE of the US.
Glantz and Noone (2000) also come up with a similar relation.

- Chuang and Penner, (1995)

They express critics about formulations reported up to now: "These parameterizations made use of measured relationships in continental and maritime clouds. However, these relationships are inherently noisy, yielding more than a factor of 2 variation in cloud drop number concentration for a given aerosol number (or for a given sulfate mass) concentration. They do not make use of information from the climate model regarding local updraft velocities, and they have had to make certain simplifying assumptions. In the study by Boucher and Rodhe (1994), simultaneous aerosol mass and CCN number concentration measurements were used to establish a hypothetical range of dependencies between the sulfate aerosol mass and the cloud drop number concentration. However, their results of the indirect radiative forcing by sulfate aerosols are sensitive to these assumed relationships and the predicted forcing may be overestimated when comparing with observations of cloud drop radius and cloud albedo. In the study by Jones et al. (1994), aerosol number concentration was related to cloud drop number concentration based on measurements. But in converting the model-predicted sulfate mass concentrations to aerosol number concentrations for use in the parameterization, the aerosol composition and the size distribution were prescribed and assumed to be universally applicable both in the case of natural background aerosol (present prior to industrialization) and in the present-day perturbed case."
They start with an assumed pre-existing particle size distribution and develop an approximation of the altered distribution after addition of anthropogenic sulfate as the superposition of three log-normal functions:

$$\frac{dN/N_{total}}{d\log\ d} = \sum_{i=1}^{3} \frac{N_i}{\sqrt{2\pi}\log\sigma_i} \times \exp\left\{-\frac{\left[\log\left(\frac{d}{D_i}\right)\right]^2}{2\log\sigma_i}\right\}$$

Values for N_i, D_i and $\log\sigma_i$ are given by them in a table, with differences between marine and continental values.
Because it is not practical to have a detailed microphysics model in a global climate model, they suggest using the parameterization of Ghan *et al.* (1993) in the form:

$$N_d = wN_a / (w + cN_a)$$

Where N_d is the cloud drop number nucleated (cm^{-3}), N_a is the background aerosol number concentration (cm^{-3}) and w is the updraft velocity (cm s^{-1}).
Instead of using the look-up table for c (as done in Hegg, 1994), they derive it directly from a microphysical model, for continental and marine cases. (See formula 4 and 5 in their article).
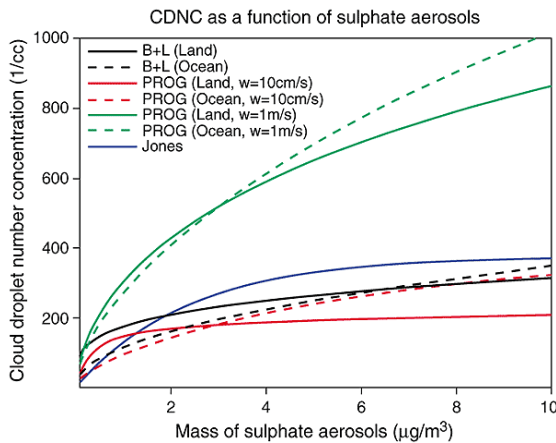

Figure 1.1 (after the IPCC report (2001)). Droplet concentration as a function of sulphate concentration for 3 different treatments: the empirical treatment of Jones et al. (1994b), the empirical treatment of Boucher and Lohmann (1995) (denoted B+L), and the mechanistic treatment of Chuang and Penner (1995) (denoted PROG).

- Feingold et al., (1996)

They predict 6 size categories of CCN, defined in terms of supersaturation, with bin bounds at 1%, .6%, .3%, .1%, .02% and 0%. The scheme is based on Twomey's (1959) relationship:

$$N_a = CS^k$$

N_a, number of activated CCN,
C and k empirically measured parameters,
S, the supersaturation

- Rotstayn, (1999)

Cloud droplet concentration, N_d, m^{-3}
Sulfate mass concentration, m µg m^{-3}

$$N_d = 10^6 \times 114.8 m^{0.48}$$
over oceans
$$N_d = 10^6 \times 173.8 m^{0.26}$$
over land

- O'Dowd et al., (1999)

Cloud droplet concentration, D (cm^{-3})
Sub-cloud aerosol concentration, A (cm^{-3})

$$D = 197\{1 - \exp(-6.13 \times 10^{-3} * A)\}$$

This parameterization is valid only at low to moderate wind speeds (1-10 m s^{-1})

- Menon, Del Genio, Koch, Tselioudis, (2002)

"We use a simple diagnostic approach to calculate N from aerosol mass based on field observations. However, we attempt to partially address the limitations of this approach by developing multiple regressions against all three simulated aerosol types (rather than assuming sulfate to be a universal proxy) and by including an empirical correction factor that mimics the effect of varying cloud turbulence strength on N." [...]
"Identical regressions are applied overland and ocean, except that sea salt is included only in the latter. The resulting multiple regression relationships to predict N for land, N_{Land}, and ocean, N_{Ocean}, are

$$N_{Land} = 10^{(2.41 + 0.50\log(Sulfate) + 0.13\log(OM))}$$ and

$$N_{Ocean} = 10^{(2.41 + 0.50\log(Sulfate) + 0.13\log(OM) + 0.05\log(Sea-salt))}$$

where sulfate, organic matter (OM), and sea salt are the mass concentrations in µg m^{-3} and N is in cm^{-3}; N predicted using the above equations is more sensitive to changes in sulfate than to OM due to the higher slope for sulfates, however, the AIE (aerosol indirect effect) has not been evaluated separately for either sulfates or OM alone."

- Abdul-Razzak and Ghan, (2004)

They review and modify/refine some of their previous relationships, obtaining this parameterization:

$$n(a_{ap}) = \sum_{i=1}^{I} \frac{N_{ai}}{\sqrt{2\pi}\ln\sigma_i} \exp\left[\frac{-\ln^2(a_{ap}/a_{mi})}{2\ln^2\sigma_i}\right]$$

where N_{ai} is the total aerosol concentration, a_{mi} is the geometric mean radius and σ_i is the geometric deviation of mode i.

- Lowenthal et al., (2004)

This article is based on recent experimental data obtained from measurements in-cloud, near cloud base, at elevated land-based sites. They derive log-log relationships between droplet concentration (CDNC, cm^{-3}) and clear air equivalent non-sea-salt sulfate (NSS, µg m^{-3}):

$$\log_{10}(CDNC) = (0.74 \pm 0.07)\log_{10}(NSS) + 2.32$$
$r^2 = 0.82$
(marine)

$$\log_{10}(CDNC) = (0.49 \pm 0.06)\log_{10}(NSS) + 2.38$$
$r^2 = 0.66$
(continental)

$$\log_{10}(CDNC) = (0.59 \pm 0.04)\log_{10}(NSS) + 2.39 \qquad r^2 = 0.81$$

(combined)

- Abdul-Razzak and Ghan, (2002)

(For the actual parameterization, see the article, equations 10-15, page 3).

About their review of available parameterization: "All previous parameterization have relied upon simplified representations of aerosol size distribution. The earliest parameterizations implicitly assumed the aerosol size distribution follows a power law. More recent parameterizations have assumed a single mode (Ghan et al., 1993; Abdul-Razzak et al., 1998) or multiple mode (Ghan et al., 1995; Abdul-Razzak and Ghan, 2000) lognormal size distribution. Although parameterizations based on such simplified aerosol size distributions accurately predict droplet nucleation when the aerosol size can be accurately approximated by the simplified representation, they cannot be expected to perform well when the aerosol size distribution is very different from the idealized form. [...] they cannot predict changes in details of the size distributions. [...] unless many narrow lognormal modes are used, the parameterizations fail to predict the sharp transition between particles large enough and those too small to be activated and the influence of the transition on subsequent aerosol activation. [...] In this paper we extend our previously developed aerosol activation parameterization for a lognormal representation of the aerosol size distribution (Abdul-Razzak et al., 1998) to a sectional representation."

- Nenes and Seinfeld, (2003)

(See the article for the actual parameterizations and definitions.) "The first attempts to relate cloud properties to aerosols in GCMs empirically linked cloud droplet number concentration to a property available in a global aerosol model, such as total aerosol sulfate mass or total aerosol number. [...] To address the deficiencies of purely empirical correlations, first-principle approaches to predicting cloud droplet number have emerged (e.g. Ghan et al., 1997; Lohmann et al., 1999). [...] Other subsequent approaches have adopted a functional relationship between the number of cloud condensation nuclei (CCN) that activate at a given supersaturation level (otherwise known as the "CCN spectrum"). [...] Other parameterizations have used lognormal representations of aerosol size distributions and have used Köhler theory[1] to compute the CCN spectrum (e.g. Ghan et al, 1993; Abdul-Razzak et al., 1998; Abdul-Razzak and Ghan, 2000). Abdul-Razzak and Ghan (2002) propose an algorithm for the use of their multiple lognormal population parameterizations in sectional aerosol models. Their approach is to use an empirically prescribed value of geometric dispersion and to treat each section as a separate mode. [...] The most sophisticated current aerosol activation parameterizations still rely on empirical information obtained from detailed numerical parcel simulations. [...] previous aerosol activation parameterizations assume one (or more) of the following: (1) specified aerosol size distributions (power law, lognormal) or a prescribed activation spectrum; (2) uniform chemical composition over particle size composed of only a completely soluble and insoluble fraction; (3) a single aerosol population (that is, an internally mixed aerosol); and (4) "instantaneous" activation of CCN (absence of kinetic effects).

- Lohmann and Feichter, (2005)

They discuss a multitude of effects (cloud albedo or Twomey effect, cloud lifetime effect, semi-direct effect, thermodynamic effect, glaciation's indirect effect, riming [adhesion of a super-cooled water droplet to an ice particle or snow crystal] indirect effect, surface energy budget effect).
They devote a paragraph to a short review of aerosol mass or number parameterizations, dividing them into two groups. "The aerosol mass or number is either empirically related to the cloud droplet number concentration (Boucher and Lohmann, 1995; Menon et al., 2002) or is obtained by using a physically-based parameterization (Abdul-Razzak and Ghan, 2002; Nenes and Seinfeld, 2003)"
They also publish graphs of the global mean Twomey effect (so called first indirect effect), lifetime effect and of global mean total indirect aerosol effects for different geographical areas (NH, SH, land, ocean, etc.) according to estimates made by different authors (that make use of different parameterizations).

The curves in figure 1.2 show graphically the amount of CCN that arises from some of the previously listed parameterizations. The parameterizations involving a single or multiple mode lognormal size distribution of aerosol are not taken in consideration any further in this study, having decided that the efforts to implement them into RACMO-2 might, at least at this stage, not be justified by the effective contribution in the improvement of the performance of the model itself. The curves show contribution of the singular terms of the parameterizations, if various types of aerosols of diverse relationships are used for different conditions. Ming et al. (2005) propose a new parameterization to link the droplet number concentration to the size distribution and chemical composition of aerosol and updraft velocity. This approach cannot be applied to our case, because we are interested in parameterizations that involve aerosol mass distribution.

Penner et al., (2004) compare the cloud optical depth required to fit the observed shortwave downward surface radiation from 2 sites, one in Oklahoma (continental polluted conditions) and the other one in Alaska (artic site, low aerosol concentration). From the good agreement between the simulated aerosol indirect effect and the observed surface radiation they conclude that the indirect aerosol effect has a significant influence on radiative fluxes.
McFiggans et al., (2005) present (among others) a review of approaches to represent aerosols in global climate models. Species taken in consideration in climate models include mineral dust, sulfuric acid, soot, sea salt, and sulfate. The most recent models also include carbonaceous aerosols. According to them there is a lack in time-resolved and accurate emissions inventories that lead to large uncertainties.
Suzuki et al., (2004), compute the number concentration of aerosol particles acting as CCN for what they consider the major aerosol species, sulfate, carbonaceous, sea salt and mineral dust aerosols.
The hygroscopic properties of (ammonium) nitrate are similar to those of ammonium sulfate and thus nitrate would in principle be a good CCN compound. However, very little is known on the size of particles in which nitrate occurs. In a separate study in this project this is investigated.

---

[1] Kohler equation governs the growth of aerosols as a function of relative humidity
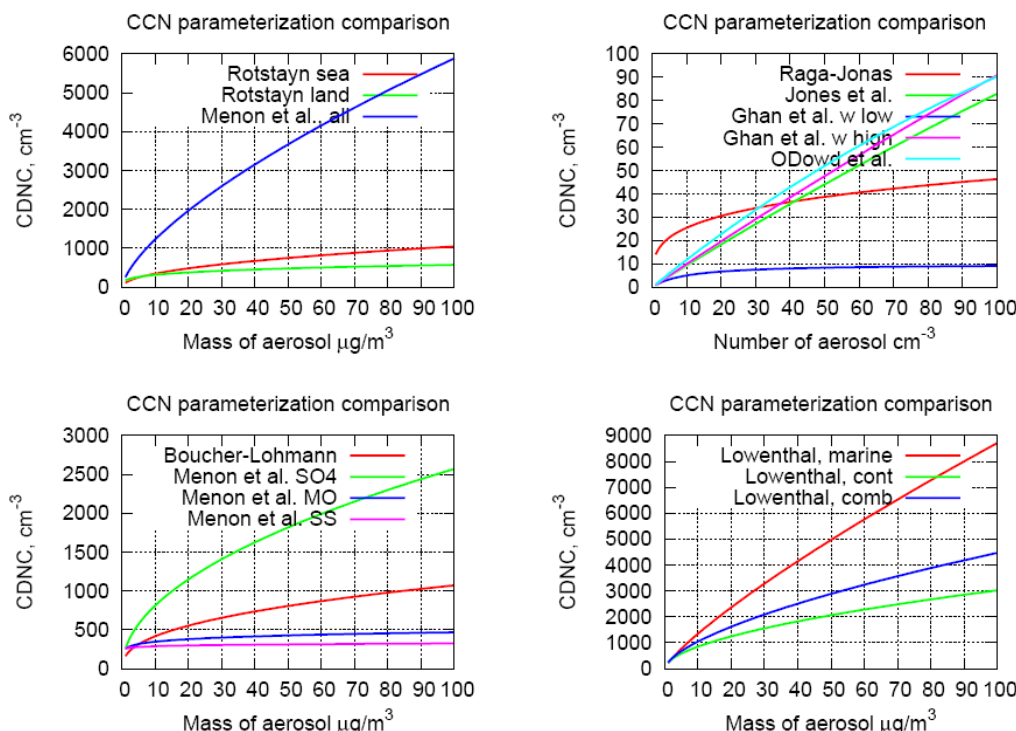
Figure 1.2 The plot in the top tight panel compares all parameterizations that use aerosol number and not mass. Because the aerosol fields used for the actual implementation of the parameterizations into RACMO2 will be provided as mass per volume, these parameterizations, even if representing some more physically based terms, have not been considered in the following.

2 Bibliographical search summary about CCN parameterizations that include nitrate

Quite some effort was put in searching for references to nitrate parameterization and in general nitrate aerosol. Despite the attempts not very much was actually found. Nitrate can be a prevalent component of cloud and fog water in Europe. A fundamental experiment in this field is the one performed in 1989 in Po-valley fog by Fuzzi et al., (1992). These authors observed that nitrate and sulfate were the major components of the aerosol soluble fraction. Together with the counter ion ammonium they account on average for 80% of the soluble fraction (the soluble part is 49% of the total aerosol mass). The Po-Valley does not constitute a unique case; there are more examples in Europe and outside. Measurements carried out at Mt. Kleiner Feldberg, Germany (Fuzzi et al., 1994) show that nitrate is an important component there as well. More recent findings in measurements at Mt. Kleiner Feldberg are reported by Elbert et al., (2000). They report that multiplication of observed levels of nitrate concentration and liquid water content result in a

nearly constant value. A comparable constant value found for the same product in data collected by others led them to conclude that nitrate derives from nitrate acting as a cloud forming agent rather than that the nitrate derives from uptake of gaseous nitric acid after the cloud has formed.

The hygroscopic properties of (ammonium) nitrate are similar to those of ammonium sulfate and thus nitrate would in principle be a good CCN compound. However, very little is known on the size of particles in which nitrate occurs. In a separate study carried out within the framework of this project this issue is investigated in more detail. Preliminary results were reported in proceedings of recent conferences and these are highly indicative of a dominant role of nitrate as CCN-agent, in the sense that the nitrate is (also) in the particles that constitute the majority of the CCN in number (See *ten Brink et al., (2007a); ten Brink et al., (2007b)*).

3 Sensitivity of cloud albedo to differences among CCN parameterizations using aerosol fields from LOTOS-EUROS model

As mentioned in the previous section, in order to keep matters simple but retain the essence, we have decided to continue this study with aerosol/cloud modules that are based on aerosol mass distributions, and avoid the complexity arising from treatments dealing with distributions dealing with aerosol number density. After a first screening four parameterizations have been selected for in-depth investigation. Specifically the following parameterizations have been further examined:

- Boucher and Lohmann, (1995), (equation D)

$$(1) \qquad CDNC = 10^{2.21 + 0.41 \log \left[m_{SO_4} \right]}$$

- Rotstayn, (1999)

$$(2) \qquad N_d = 10^6 \times 114.8 m^{0.48} \quad \text{(ocean)}$$

$$(3) \qquad N_d = 10^6 \times 173.8 m^{0.26} \quad \text{(land)}$$

- Menon et al., (2002)

$$(4) \qquad N_{\text{Land}} = 10^{(2.41 + 0.50 \log(\text{Sulfate}) + 0.13 \log(\text{OM}))}$$

$$(5) \qquad N_{\text{Ocean}} = 10^{(2.41 + 0.50 \log(\text{Sulfate}) + 0.13 \log(\text{OM}) + 0.05 \log(\text{Sea-salt}))}$$

- Lowenthal et al. (2004)

$$(6) \qquad \log_{10}(\text{CDNC}) = (0.74 \pm 0.07) \log_{10}(\text{NSS}) + 2.32 \qquad r^2 = 0.82$$
(marine)

$$(7) \qquad \log_{10}(\text{CDNC}) = (0.49 \pm 0.06) \log_{10}(\text{NSS}) + 2.38 \qquad r^2 = 0.66$$
(continental)

All four parameterizations consider aerosol quantities as µg/m³. Apart from the first, they all make a distinction between sea and land cases. Only the one by Menon et al. includes also organic matter and sea-salt, while all the others regard sulfate aerosol as representative of all aerosol species. Note that the equations (6) and (7) have been modified adding the brackets around the two first terms, having found a typing error in the way they where reported in the article by Lowenthal et al., (2004).
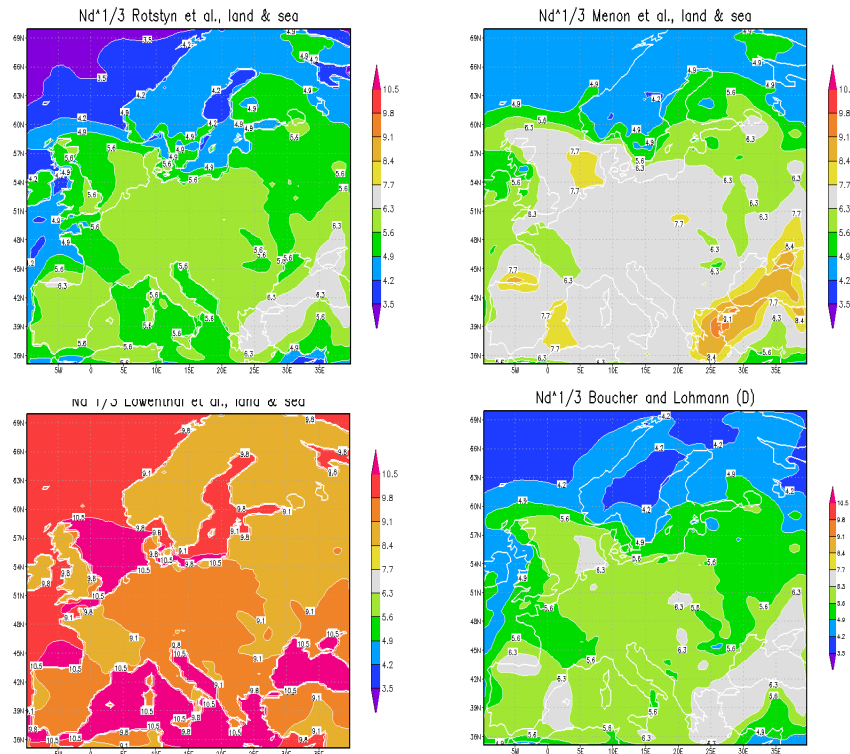

Fig. 3.1 – *Cubic root of the cloud condensation nuclei number, proportional to the optical thickness for parameterizations 2-7. Same colorbar, for an easier comparison.*

It is interesting to see how relations (1)-(7) display geographically. To study this, we have looked at spatial distributions produced by the LOTOS-EUROS model, hereafter reported to as LOTOS. This is a chemistry-transport model developed and operated by TNO (Netherlands Organization of Applied Scientific research) (Schaap et al., 2005). The LOTOS model grid and domain consist of a rectangular regular mesh with a spatial resolution of 0.5x.25° lon-lat, covering the area between 10°W and 40°E and 35° to 70°N (all Europe). Meteo-forcings to LOTOS are provided by an atmospheric model, e.g. ECMWF analyses or a time series from RACMO. Relationships (1)-(7) have been computed using the values of aerosol from LOTOS simulations covering the months of May and August 2000. More specifically, the values of sulfate are those directly computed by LOTOS, the values of sea salt have been calculated from the LOTOS sodium (fine amount). Organic matter is not among the LOTOS output, so it has not been taken in consideration in the two formulas by Menon et al. Whenever parameterizations have a distinction between sea and land, the appropriate formula has been applied to sea and land grid points

respectively. Plots in figure 3.1 represent the results of the four parameterizations on the first day, first time step of the month of August 2000, for the lowest LOTOS model level, expressed in the cubic root of the cloud condensation nuclei number (This value is proportional to the optical thickness). To better compare among the different parameterizations all values have been plotted within the same range of values (same colorbar interval).

This type of comparison clearly shows how the parameterization by Lowenthal et al. (2004), ranging from 8.8 to 10.8, is well above the values of the other two. Rotstayn (1999) has the lowest values, from 3.6 to 6.6, while Menon et al. (2002) presents the broadest variation, from 4.25 to 9.25, even if most of the points of the LOTOS domain fall around the value of 6.25. It is also evident that quite high values of $Nd^{1/3}$ are found in the south east corner (SE area) of the domain in all parameterizations. This effect is clearly connected to the use of the sulfate alone as source of cloud condensation nuclei. To demonstrate this, the output of LOTOS for SO_4 and Na on monthly average for the months of May and August 2000 are reported in figure 3.2.
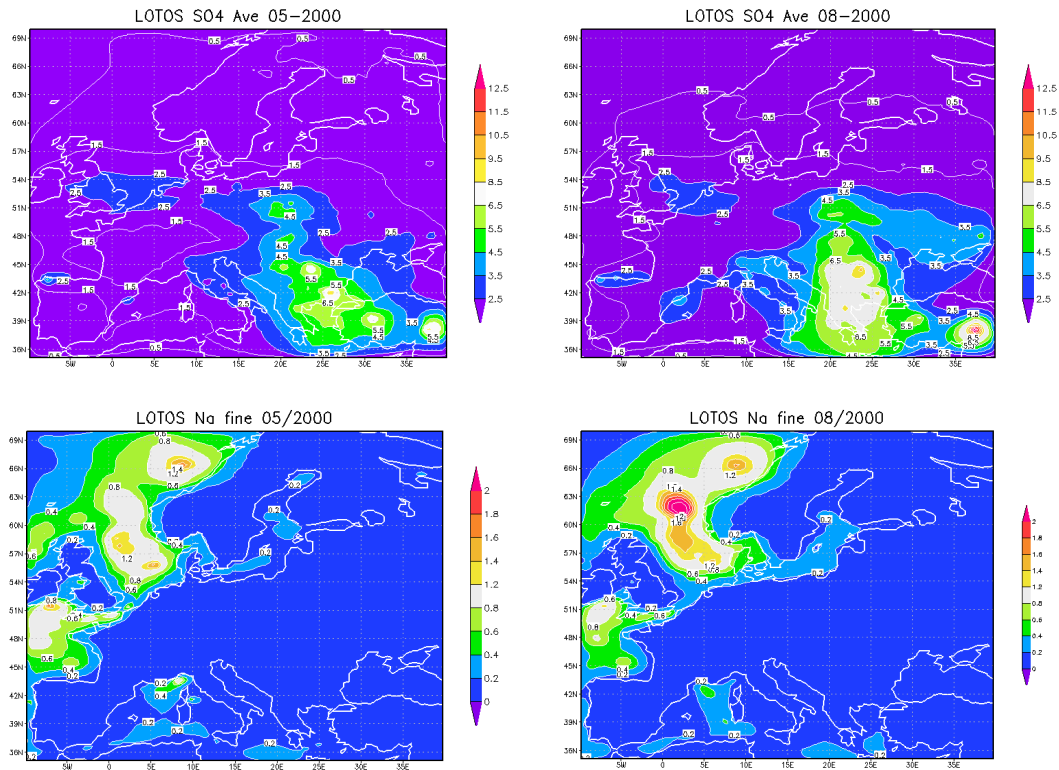

Figure 3.2 – *LOTOS output data, monthly average: Sulfate (top) and Sodium (bottom) for May (left) and August (right) 2000, surface layer.*

It is clearly visible how the sulfate concentration peaks in the SE area of the domain, and that sea salt does not contribute to the effect. It is also evident that these are a kind of persistent features that do not show up 'accidentally' just on a short period of time.
Another quite striking feature (Figure 3.1 again) is in the Lowenthal et al. (2004) parameterization, where almost all sea points show higher values than the land points. This comes out from the parameterization expressions (6) and (7) and it is directly connected to the way those authors fitted their dataset, and ultimately to the dataset itself.

To get a more quantitative and physically based comparison among all four parameterizations considered in this study, differences in aerosol between the relation by Boucher and Lohmann (1995) (taken as the reference one) and the other three have been computed following the strategy explained below.

The aim of the exercise is to obtain differences in the form $\Delta A = A_{BL} - A_i$, where A is the albedo, *BL* denotes the Boucher-Lohmann parameterization (1) and *i* can be one of the other parameterizations (2)-(7). Following the article by King and Harshvardhan (1986), using the so called two-stream

● ● ● ●　　　6　Sensitivity of cloud albedo to differences among CCN parameterizations using aerosol fields from LOTOS-EUROS model

approximation, it is possible to write the plane albedo (indicated by $\hat{r}$ in the original paper) as function of the total optical depth τ_t and the solar zenith angle μ_0

$$\hat{r}(\tau_t, \mu_0) = 1 - \hat{t}(\tau_t, \mu_0) = \frac{1}{1 + \gamma_1 \tau_t}\left[\gamma_1 \tau_t + (\gamma_3 - \gamma_1 \mu_0)\left(1 - e^{-\tau_t/\mu_0}\right)\right]$$
(*)

In the above relation the γ's represent coefficients that take different forms according to different authors.
In the approximation by Coakley and Chýlek (1975) they are expressed as functions of the backscatter fraction, $\beta(\mu_0)$, the solar zenith angle μ_0 and the scattering ω_0:

$$\gamma_1 = \{1 - \omega_0[1 - \beta(\mu_0)]\}/\mu_0 \ ; \ \gamma_2 = \omega_0\beta(\mu_0)/\mu_0 \ ;$$
$$\gamma_3 = \gamma_1\mu_0 = \beta(\mu_0)$$

Substituting in (*), in the case of conservative scattering, for which $\gamma_1 = \gamma_2$, one gets an expression of the albedo as combination of the scattering and the total optical depth:

$$\hat{r}(\tau_t, \mu_0) = \frac{\gamma_1 \tau_t}{1 + \gamma_1 \tau_t}$$
(**)

Now, the optical depth can be expressed as function of the cubic root of the cloud condensation nuclei number, N_d, as follows:

$$\tau = \frac{3}{2}\frac{LWC \cdot \Delta z}{r_e} \ , \ \text{with} \ r_e \cong \left(\frac{3}{4\pi}\frac{LWC}{\rho N_d}\right)^{1/3} \ , \ LWC \text{ liquid water}$$

content, r_e effective droplet radius, ρ density and Δz cloud thickness.

The generic difference of albedo between the one as computed using the expression for N_d by Boucher and Lohmann (1995) (hereafter denoted by 'BL') and the albedo as computed using one of the other expressions (2)-(7) for N_d (hereafter denoted by 'other') can be thus be written as:

$$\Delta A = A_{BL} - A_{other} = \frac{\gamma\tau_{BL}}{1 + \gamma\tau_{BL}} - \frac{\gamma\tau_{other}}{1 + \gamma\tau_{other}}$$

Assuming that $\tau_{other} = \tau_{BL} + \Delta\tau$, after Taylor expansion and other substitutions one gets:

$$\Delta A = A_{BL} - A_{other} = A(1 - A)\frac{1}{3}\frac{\Delta N}{N} \ , \ \text{with} \ \Delta N = N_{BL} - N_{other}$$

The factor A(1-A) has a maximum value of 0.25 for A=0.5. This means that the maximum difference in albedo as function of the cloud condensation nuclei number can be expressed as follows:

$$\Delta A_{max} = \frac{1}{12}\frac{N_{BL} - N_{other}}{N_{other}}$$
(8)

Formula (8) has been computed for all the different parameterizations of N_d on each point of the LOTOS domain.

The plots of figure 3.3 show the monthly averages of maximum difference in albedo for August 2002. The BL - Rotstayn albedo difference spans from -0.025 in the continental north area to 0.025 over coastal areas, with a large continental part of the domain showing no differences. The BL - Menon albedo difference presents everywhere negative values (from -0.0725 to -0.0225), indicating that the Manon values are always greater than those computed from the BL formula. Moreover, they also fall below the lowest value of the BL- Rotstayn albedo difference. As expected, the BL - Lowenthal shows the biggest differences in this set of albedo comparisons. Values range from 0.05 in the NW sea area to -0.15 on small spots in the Aegean Sea. Most of the land points show a difference in albedo (-0.7) larger than those found for the other two cases. Note that the three plots each have attached a different color bar range. It is pointed out that the approximation used in this study to assess the difference in albedo is valid only when the optical depth values of the compared parameterizations are quite similar, so in principle should not be applicable to the BL-Lowenthal case. Moreover plotting the maximum possible differences instead of the mean differences in albedo tends to overemphasize the effect. Probably, in general, differences will be not that big.
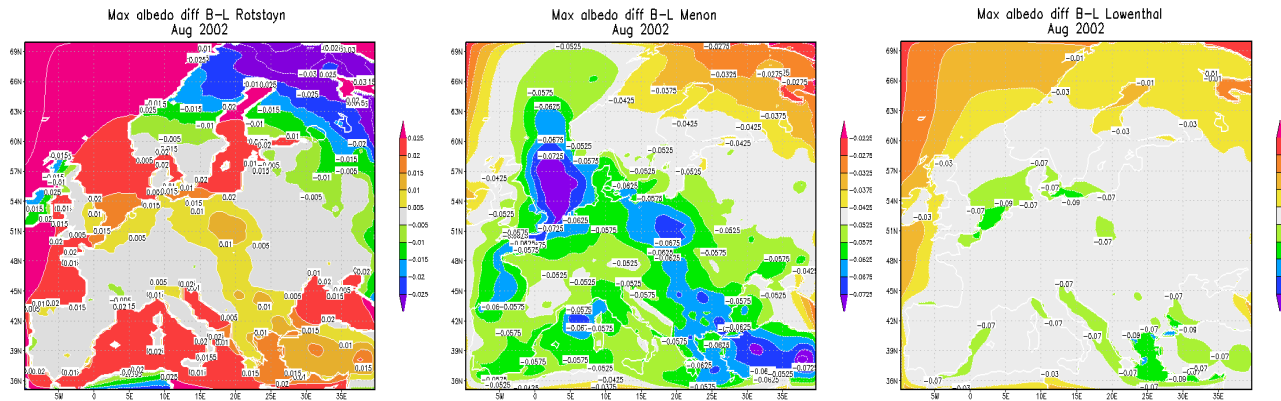

Figure 3.3 – *Maximum possible difference in albedo: monthly average for August 2002. Different colorbars are used to show the complete range of variation for each comparison.*

● ● ● ●   7   Sensitivity of cloud albedo to differences among CCN parameterizations using aerosol fields from LOTOS-EUROS model

4   Sensitivity of cloud albedo to the use of different CCN parameterizations

Aerosol fields used in this sensitivity study have been computed with the chemistry-transport model LOTOS operated by TNO. The data base consists of hourly values for the complete year 2002, based on runs with LOTOS driven by the meteorological data obtained from ECMWF operational analyses. The following species are available: SO_2 [ppb], HNO_3 [ppb], NH_3 [ppb], SO_4a [µg/m3], NH_4a [µg/m3], NO_3a [µg/m3], where 'a' stands for aerosol, in the `le_conc_'month'.dat` files, and bc [bc], pm25 [µg/m3], pm10 [µg/m3], na_f [µg/m3] and na_c [µg/m3], where _f is 'fine' and _c is 'coarse', in the `le_pm_'month'.dat` files.
All species have been computed at the five vertical levels employed by LOTOS (from above the surface up to 5 km).

The aerosol fields have been used as input to the four different parameterizations introduced in Section 3, equations (1) – (7), in order to compute CCN. These parameterizations are as stated before those by Boucher and Lohmann, (1995), (their equation D); Rotstayn, (1999); Menon, Del Genio, Koch, Tselioudis, (2002); Lowenthal et al. (2004).
The actual computations are performed by modules, included in a FORTRAN 90 routine (`ccn_simple.f90`). For each parameterization, the routine computes the corresponding value of CCN.
A number of post processing computations has been performed. First, the maximum possible difference in albedo has been computed for each parameterization with the one by Boucher and Lohmann serving as a reference. A monthly mean has been computed, and using appropriate values of the solar zenith angle, an area mean has been determined. Results are shown in the plots of figure 4.1, taken from a poster presentation for the EGU 06 Conference (De Martino et al., 2006). At an arbitrary instant in time, for example at 12 UTC on 15 August 2000, the differences in domain averaged albedo are $3.26e^{-2}$ for the comparison BL - R, $2.15e^{-2}$ for the BL - M one, and $3.79e^{-2}$ for the BL - L one. For any specific time instant of the year, the differences in domain averaged albedo are found to be greater than 2% in all cases considered. Such values reflect the uncertainty in albedo computation on which typical estimates of the aerosol indirect effect are made.

In order to obtain maximum possible differences in terms of radiation, the following formula have been used

- Irradiance at the ith grid cell:
$$R_i = \alpha_i \mu_o S_o$$

- Differences in irradiance:
$$\Delta R_i = \Delta \alpha_i \mu_o S_o$$

- Differences in irradiance at t_j:
$$\Delta R_i(t) = \Delta \alpha_i(t) \mu_o(t) S_o \qquad [Wm^{-2}]$$

- Differences in irradiance at t_j over an area:
$$\Delta R_i(t) B_i = \Delta \alpha_i(t) \mu_o(t) S_o B_i \qquad [W]$$

- Total domain average in differences in irradiance at t_j:

$$\frac{\sum_i \Delta R_i(t) B_i}{\sum_i B_i} = \frac{\sum \Delta \alpha_i(t) \mu_0(t) S_0 B_i}{\sum B_i} \qquad [Wm^{-2}]$$

where: i = index of grid cell; j = index of time; A_i = albedo of the ith grid cell; B_i = area of the ith grid cell; Δt_j = time interval 'around' time with index t_j.
Once computed all µ's for each location and each time step, and the partial and total areas, the last formula has been applied to compute daily time series of the maximum differences in irradiance for the various parameterizations, once again with the parameterization proposed by Boucher and Lohmann serving as a reference.
The results are shown in figure 4.2. A seasonal signal is evident in all three comparisons, while the smaller perturbations are due to the changes in concentrations of aerosols and related CCN values during the year. The reported results are based on the implicit assumption that a stratocumulus layer is present all the year long, over the complete domain. This is an unrealistic assumption, of course. To get a realistic picture of maximum differences in radiations that can arise just using different parameterizations of CCN, one should use realistic cloud fraction and daily cloudiness values. This can be done, using for example data from a RACMO-2 run. Results are expected to be in the range of 3-4 W/m².
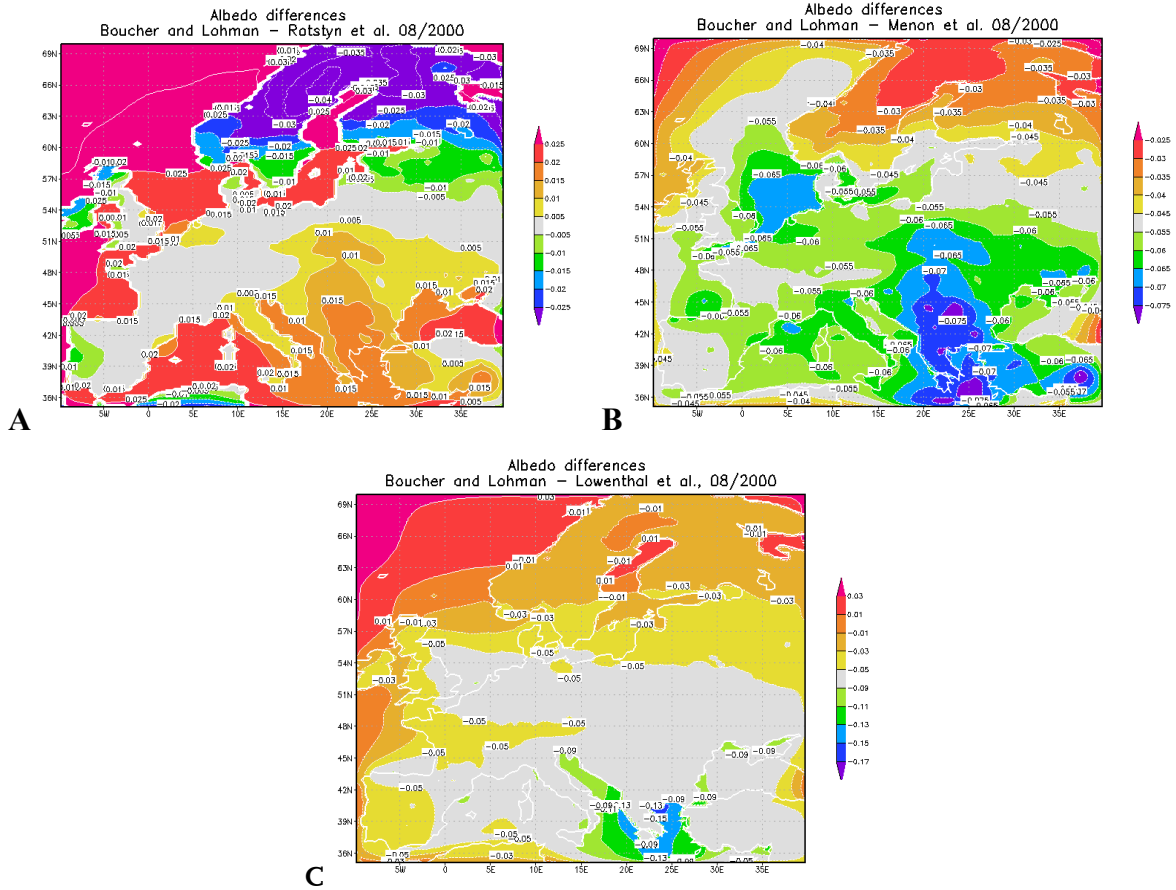
Figure 4.1 - *Maximum possible difference in albedo, plotted on the LOTOS domain between the formulation proposed by Boucher and Lohmann, (1995) and the one by Rotstayn (1999) [panel A]; between Boucher and Lohmann, (1995) and Menon et al. (2002) [panel B]; between Boucher and Lohmann, (1995) and Lowenthal et al. (2004) [panel C], based on aerosol data for August 2000.*
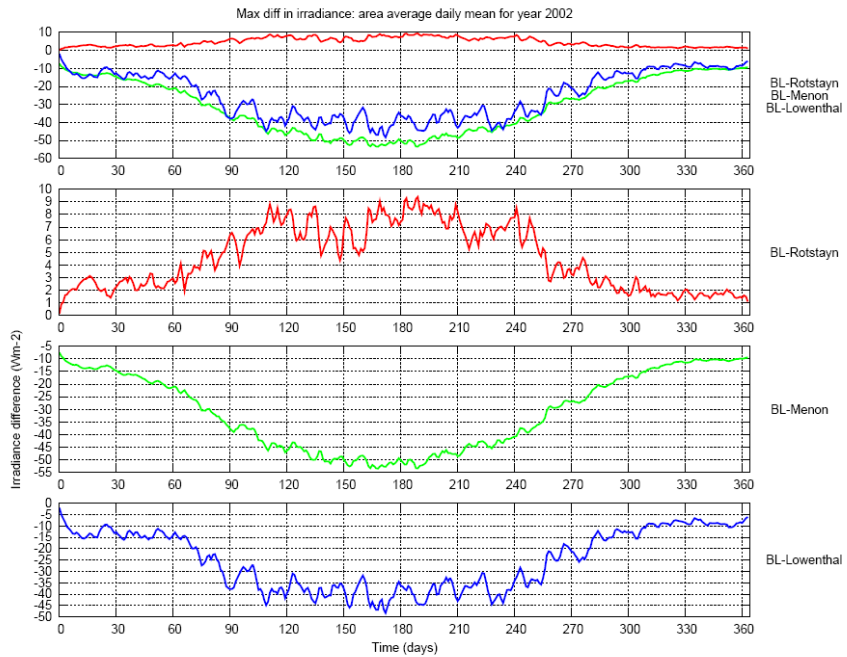

Figure 4.2 – *Maximum differences in irradiance for the whole year 2002: area average.*

Sensitivity of cloud albedo to the use of different CCN parameterizations

5   Evaluation of specific CCN parameterizations in the framework of the RACMO2 radiation module

The objective of the evaluation is to assess the performance of the new CCN modules after implementation in the radiation module of the Regional Climate model RACMO2. The actual runs are carried out with the radiation module of the single column (SCM) version of RACMO2. The impact of using different parameterizations to the radiation at the surface and at the top of the atmosphere, the impact of using constant (averaged over the day) or time varying aerosol concentrations, the effect of using either the homogeneous or the inhomogeneous mixing scheme, both schemes respectively assuming an effective radius that is either constant or varying with height, the impact of the K factor (relation between the geometric radius and the effective radius), the effect of different switches/schemes activated/not activated in the SCM (more details about these last tests in the following) are the topics of this section. The motivation for the choice of these four CCN parameterizations (B-L, L, M and R) has already been discussed in a previous section.

The evaluation is entirely based on observations collected at the Cabauw site (51.97N, 4.93E) on 30 January 2007 This specific date is chosen because it is the only day (so far) for which a comprehensive set of measurements is found to be available including both meteorological parameters and aerosol loadings, this in combination with the occurrence of favorable cloud conditions, namely a thin deck stratocumulus persisting throughout the day. The radiation module is forced with observed meteorological parameters, including surface pressure, and thermodynamic profiles of temperatures, specific humidity and liquid water content (LWC) obtained from IPT retrievals (Löhnert et al, 2004). A compilation of the observed time series is shown in Fig 5.1. According to the cloud classification displayed in the upper panel there was a persistent cloud deck throughout the day with cloud base at 1000 m and thickness in the order of 300 m. The rain detector mounted onto the microwave radiometer

(HATPRO) nor the standard rain gauge reported any rain that day reaching the surface. Although difficult to discern from Fig. 5.1, we like to point out that the liquid water path (LWP) derived from the IPT retrievals is found smaller than the value obtained with the standard statistical algorithm applied to HATPRO, in particular when absolute values are small, e.g. between 10 and 15 UTC. This discrepancy will potentially have repercussions in the analysis of the evaluation.

Similar to the meteorological parameters, aerosol observations have been used to drive the CCN module. Figure 5.2 shows time series of hourly inferred aerosol loadings of two aerosol types, i.e. non sea-salt sulfate (NSS) and sea-salt, as measured by MARGA, an instrument for Measuring AeRosol and Gases. The wind turns from W to SW, and this causes the reduction of the amount of sea-salt aerosol and the increase of sulfate in the course of the day in the column of measurement. To evaluate the response of the radiation module we have focused on the short wave radiation. The model short wave incoming radiation at the surface is compared with measurements of global radiation at the BSRN (Baseline Surface Radiation Network) site Cabauw. The model short wave reflected radiation at the top of atmosphere is compared with GERB observations (Geostationary Earth Radiation Budget).

Based on the meteorological and aerosol input described above the amount of CCN produced by all four parameterizations is shown in Fig. 5.3. The parameterizations can be subdivided into two groups: the ones by B-L and R that give a lower amount of CCN (between 100 and 250 Nd/cm^3) and those by M and L that give a higher amount of CCN (between 150 and ~400 Nd/cm^3). In some of the tests reported in the following, for brevity, just one representative of the first group (B-L) and one of the second group (M) is taken into consideration in the comparisons.
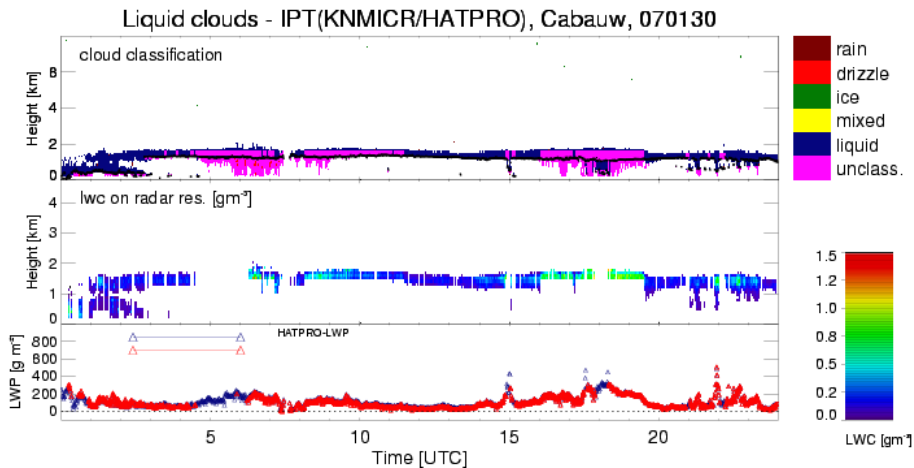

Figure 5.1 - IPT data for the 30 January 2007. One single layer of cloud is present over the whole day.
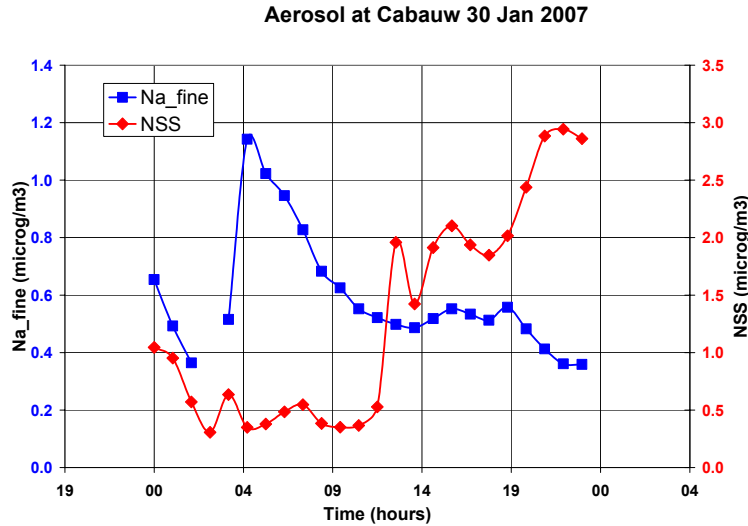
Figure 5.2 - *Hourly values of aerosols, 30 January 2007, for Cabauw as measured by MARGA.*
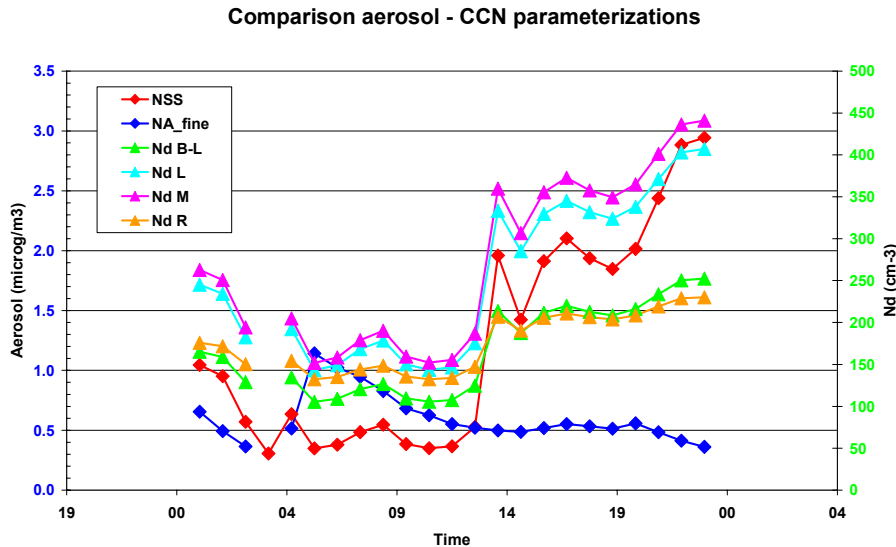

Figure 5.3 - *Amount of CCN as obtained applying the four different CCN parameterizations on the MARGA aerosol data.*

5.1 Evaluation with daily averaged aerosol (AVE)

First, the hourly values of measured aerosol have been averaged over the 24 hours of 30 January 2007. The resulting values of 1.3 μ/m³ for NSS and 0.62 μ/m³ for Na_fine have been used in the numerical experiments. In this specific test the meteorological input is taken from the IPT retrievals that are closest to the half hour (for example, the IPT retrieval closest to 11:30 provides the input of a run at 11:30, which in this evaluation is considered representative of the interval 11-12 UTC. Given the presence of invalid data in the IPT fields, the actual time used can differ a few minutes with that half hour). For each daylight hour, the bars in Fig. 5.4 show the difference in incoming SW radiation at the surface

between the B-L parameterization and any of the other three parameterizations. The difference can be up to ~8W/m² depending on absolute incoming short wave radiation and CCN parameterization.

The figure 5.5 shows the comparison of the radiation at the surface with the BSRN data and at the TOA with the GERB data, respectively. Quite large differences are present, especially in the central part of the day. The model overestimates the incoming radiation at the surface and underestimates the one going up at the TOA. The hours with the poorest results correspond to a very low value in the LWC, showing that the model in its standard configurations has troubles in handling thin clouds. This point will be further investigated in the model runs made using all the time steps.
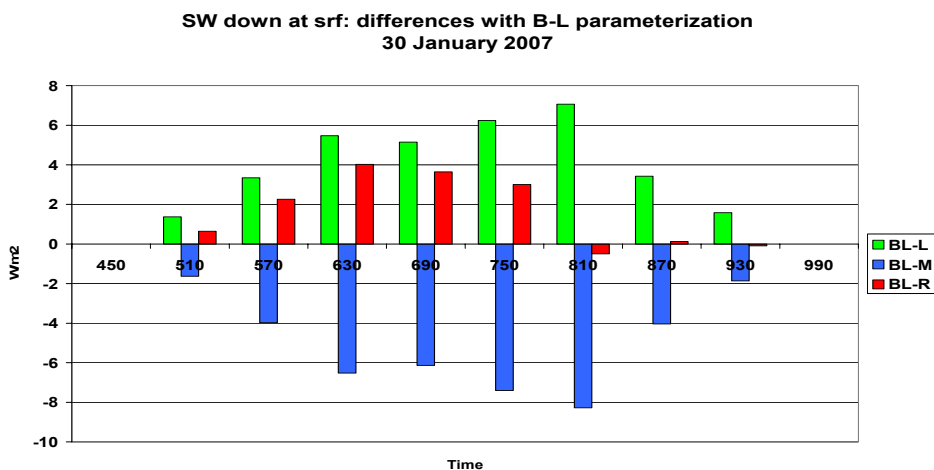
● ● ● ●   11   Evaluation of specific CCN parameterizations in the framework of the RACMO2
radiation module

**SW down at srf: differences with B-L parameterization
30 January 2007**

Figure 5.4 - *AVE test: radiation at the surface and relative differences.*
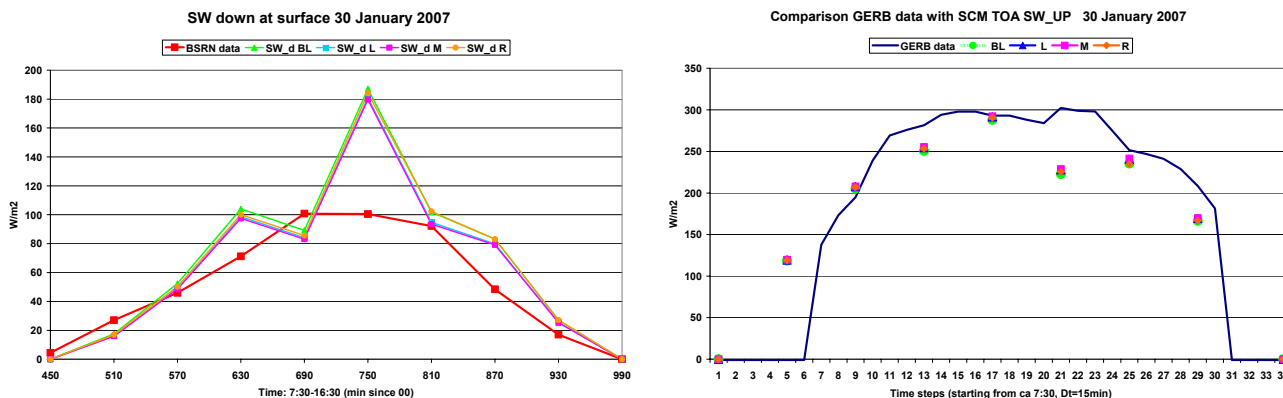
Figure 5.5 - *Comparison with data of the radiation output.*

Nd interpolated and average aerosol
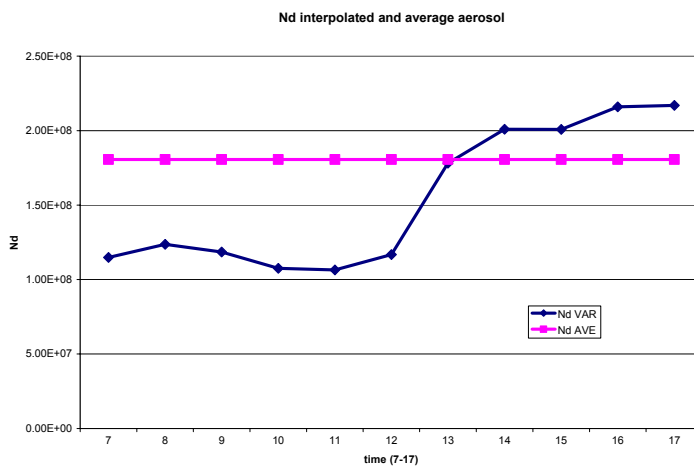

Figure 5.6 - N_d *computed using the B-L parameterizations for the AVE and the VAR tests.*

● ● ● ●   12   Evaluation of specific CCN parameterizations in the framework of the RACMO2
radiation module

5.2 Evaluation with time-varying aerosol(VAR)

For the runs discussed in this paragraph, the MARGA inferred aerosol data have been linearly interpolated to the exact time values of the IPT profiles (that are available at a frequency of more than one value per minute). The N_d time series resulting from the time varying and the daily mean aerosol amounts using the parameterization by B-L are shown in Fig. 5.6.

The curves in Fig. 5.6 show that the computation in the radiation module has been performed using the value of $N_d=180$cm^{-3} in the case of AVE, and values between 100 and 230 for the VAR tests (and B-L parameterization, for example).

5.2.1 Effect of different parameterizations

Using the same standard settings of the switches in the radiation module, the inhomogeneous mixing scheme (assuming that the effective radius varies with height), and a K factor of 0.95 (relationship between geometrical droplet radius and effective radius), the role of using parameterization schemes yielding high (M) or low (B-L) values of CCN has been examined. The effect on incident short wave radiation at the surface and reflected radiation at the TOA is shown in Fig 5.7. The parameterization by B-L, starting from less N_d, gives higher radiation at the surface and less at the TOA compared with the results using the M parameterization. The differences are (in absolute values) about 7 W/m² in both cases.
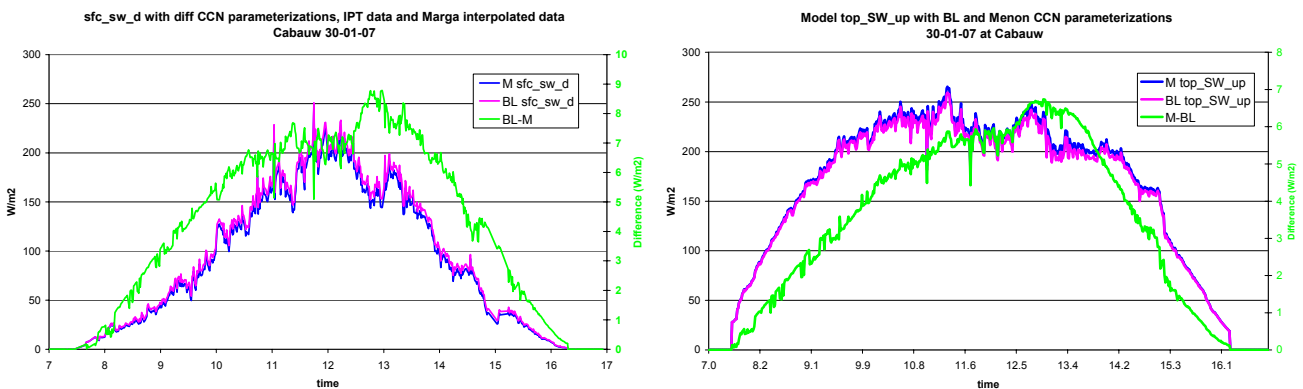

Figure 5.7 - *Left: Incoming SW radiation at the surface using two different parameterizations (blue and violet) and mutual differences (green). Right: SW going up at the TOA as computed using two different parameterizations (blue and violet) and mutual differences (green).*

5.2.2 Effect of constant and time varying aerosol field (AVE vs VAR)

Keeping the CCN parameterization unchanged (B-L in the case shown) and fixing all other model settings, the effect of using an averaged aerosol value over the whole day and the time varying data has been investigated. Results, illustrated in Fig. 5.8 for the incoming SW at the surface, show that the difference is in the same order of magnitude (~ 10 W/m2) as the one found in the previous paragraph using different CCN parameterizations.

5.2.3 Model output compared with data

The short wave radiation at surface and TOA as it is computed by the radiation module in response to the forcing, has been compared with observations. For the comparison at the surface the BSRN data have been used, and more specifically the parameter referred to as DSGL2 (which is slightly different from DSGL1, but it is supposedly more precise, because some corrections have been applied). The file BSRN_0812_20070130.txt contains all the available data for the 30 January 2007 measured at Cabauw. There are 1440 time steps; this means 60 values per hour, one value each minute. For

the comparison at the TOA the GERB data have been used, already specifically post-processed to be representative of Cabauw. The file Cabauw_200701_V003.txt contains data for the whole month. For 30 January 2007 there are 92 time steps in total. In general, data are available each 15 min (starting at 00:00, and then 00:15, 00:30, 00:45, 01:00, etc.). The values at 15:00, 15:15, and 15:30 are missing. The real time of the measurement is in the first column of the file, and can deviate from the exact time. The SW radiation value needed for the comparison is the solar flux denoted as flux_s.

Fig 5.9 shows the comparisons between the model output (in blue and purple for the B-L and M parameterizations respectively) and the data (in red) for the SW at the surface and at the TOA.

Evidently, the matching in an absolute sense is quite poor with differences reaching almost 100% in the central part of the day . Recognizing that there exists a general consensus on the quality of the BSRN and GERB data, the source of the error(s) has to be searched elsewhere. The following paragraph discusses all the checks that have been performed on the IPT input data, on the way they have been imported into the model, and on the model settings, in the hope of improving the comparison.
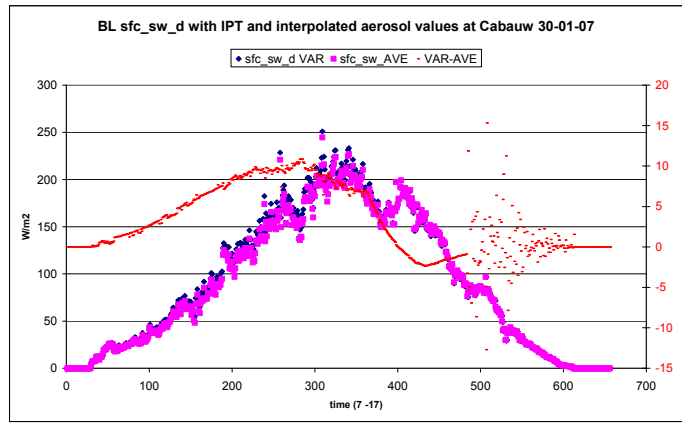
● ● ● ●   13   Evaluation of specific CCN parameterizations in the framework of the RACMO2 radiation module

Figure 5.8 - *Incoming SW at the surface: same parameterization (B-L), different CCN fields computed using a constant or time varying aerosol concentration. The red line displays the difference in CCN derived with constant and time varying aerosol.*
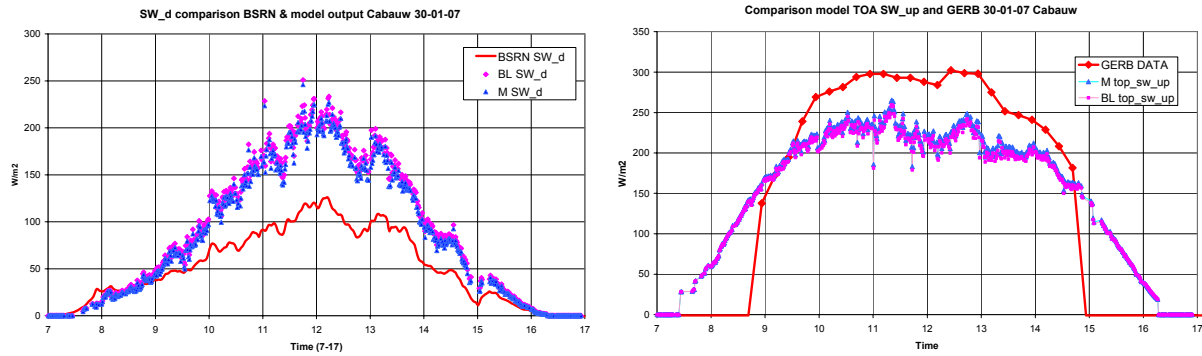

Figure 5.9 - *Left: Model incoming SW at the surface compared to BSRN data; right: model outgoing SW radiation going out at the TOA compared with GERB data.*

5.3 Improving the comparison with surface data through changes in the model settings

First, we performed some checks to rule out the presence of any trivial errors. The solar zenith angle dependent on the coordinates of the column, the date and the daytime hour has been checked and found correct. The IWV and LWP values of the model profiles resulting from projection of the IPT profiles at model resolution have been compared with the original column values at IPT resolution. The majority of values was found to match very well, although a small amount of scatter remained present, however by far not enough to explain the huge overestimation of the model in representing the incident short wave radiation at the surface.

Next, the settings of the radiation module have been checked. The cloud layer observed on 30 January 2007 was quite thin, and for most of the time it occupied just one model layer, or at most two layers. This means that it is likely reasonable to assume that the effective radius does not vary with height, so that the homogeneous mixing scheme can be safely used for this case. Moreover the amount of available aerosol justifies the use of a quite high K factor (chosen as 0.95). The curves in figure 5.10

show the sensitivity of the model to the different mixing schemes and K factors. It is clear that the combination of homogeneous mixing and setting K to 0.95 yields the best result (pink curve), lowering the amount of incoming SW at the surface, and bringing it closer to the data. For brevity, only the period 11 - 12 UTC has been investigated, when the differences between modeled and observed incident short wave radiation are found largest. In the same Figure the black curve represents the response of the control version of radiation module without the new CCN modules. Here, also the sensitivity to the number of model layers is examined 40std and 60std refer to 40 and 60 model layers, respectively. The result show nearly identical results for the two vertical meshes.

In all model results discussed so far the liquid water amounts have been reduced by 70% prior to calculating the response of the radiation module. This so called inhomogeneity factor is meant to correct the radiative flux calculation for the assumed shortcoming that the radiation module does not account for horizontal

variations in cloud water amounts, but only acts on the mean state. However, application of this factor is redundant in the context of this calculation because the IPT measurements must be regarded as point measurements with negligible horizontal scale, whereas the spatial variations are implicitly contained in the IPT time series. Moreover, it is argued by De Roode and Los (2008), based on evidence obtained with LES, that even

for larger horizontal scales the value of the inhomogeneity factor is much closer to 1., at least larger than 0.96. In fact, the used value of 0.7 can be considered as an attempt applied in past versions of the ECMWF model to correct for the tendency to substantially overpredict LWP.
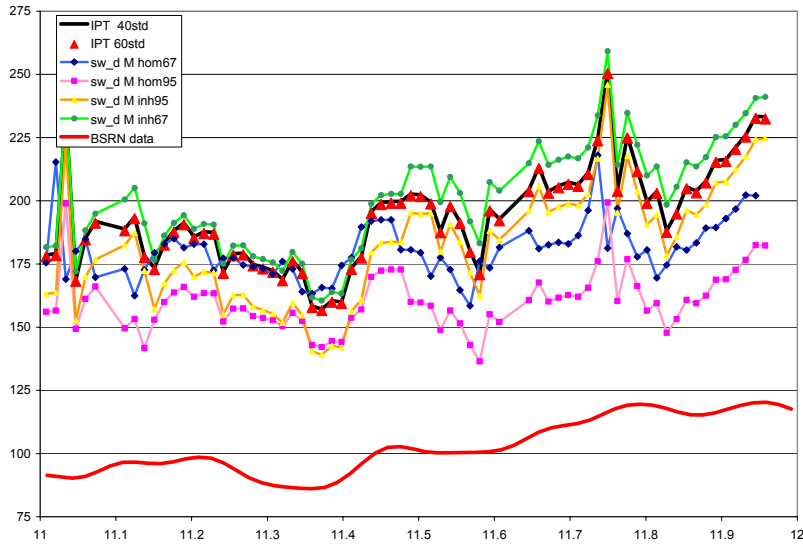

Figure 5.10 - Sensitivity to the mixing scheme and the K factor.

This adjustment substantially improves the comparison with observations, as can be seen in Fig. 5.11 (left panel, light blue curve). In the same figure (right panel) the effect of artificially doubling the amount of LWC is shown for the version with the standard radiation module (no new CCN modules, inhomogeneity factor 0.7; black curve), and for the version with the Menon CCN parameterization (pink curve).
Figure 5.12 shows the comparison between model output and observations when both the inhomogeneity factor is switched off, and the hom95 setting is used, retaining the LWC amount as it is provided by the IPT retrieval (yellow

line, in contrast with the pink one with the inhomogeneity factor turned on).
The standard SCM cycle 31r1, in which the new CCN parameterizations and effective radius modules have been implemented, is based on application of an old SW scheme, which has been the default in many previous cycles, including cy23r4 (ERA40), supplemented with an updated aerosol climatology to account for the aerosol direct effect. Putting back the old climatology (LNEWAER_F) the comparison with the surface radiation data improves even more, as is shown by the blue curve in Fig. 5.13. This is the best comparison that can be obtained without modifying the input data.
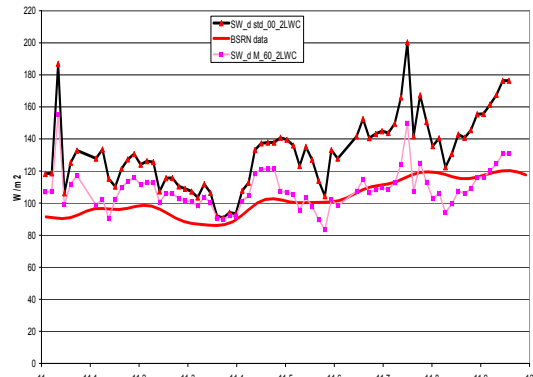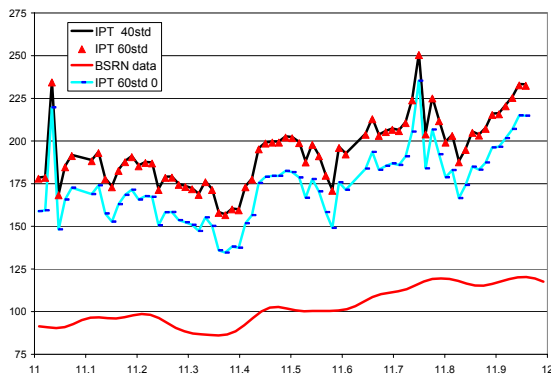

Figure 5.11 - Left: effect of setting off the model inhomogeneity factor; right: effect of artificially doubling the LWC.
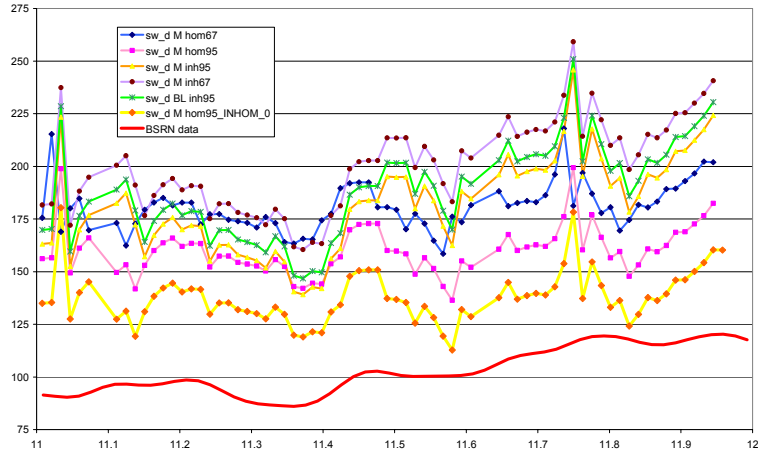
● ● ● ●   15   Evaluation of specific CCN parameterizations in the framework of the RACMO2 radiation module

Figure 5.12 - *Incoming SW radiation at the surface between 11 and 12 UTC on the 30 January 2007: comparison between different model settings and data.*
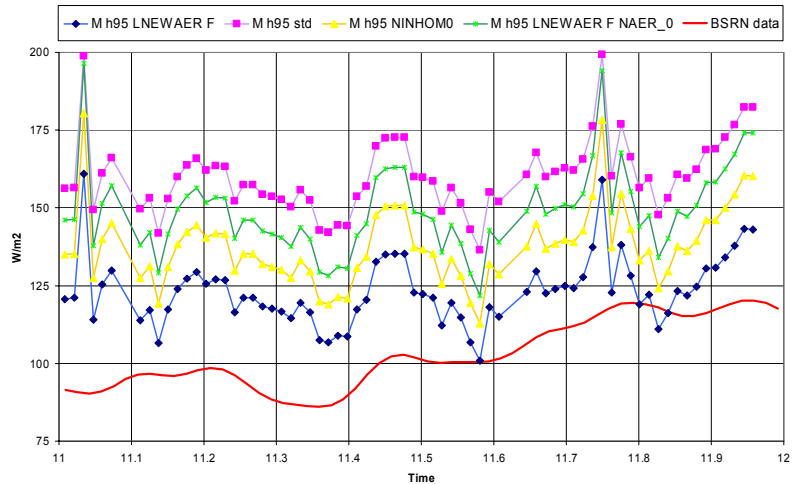

Figure 5.13 - *The blue curve is the best results without modifying input data.*

5.4 Improving the comparison with surface data through changes in the input

The experiment with doubled LWC (see figure 5.11, right panel) shows that the model is quite sensitive to the value of LWC. The underlying question is whether the remaining difference between model output and data is due to a problem in the radiation module or in the input data, or both. Fig. 5.14 shows the time series of the input LWP derived from the IPT retrieval. From 10 to 14 UTC the values are below 100 g/m², and even below 50 g/m² around 12 UTC.

Moreover, the comparison between the IPT retrieval and the result obtained with a standard statistical retrieval algorithm to infer LWP from HATPRO measurements shows that LWP derived from the IPT retrieval is mostly below the statistically retrieved value, in particular at low amount of LWP, e.g. between 11 and 14 UTC, when the

reduction factor reaches values between 25 and 50% (Figure 5.14, compare the red (IPT), with the other two curves). To examine the sensitivity to this apparent discrepancy we have loaded the radiation module with a sequence of modified IPT retrievals in which the LWP value is corrected to match the statistically retrieved LWP value while the shape of the vertical profile has been retained. The result is shown by the light blue curve in Fig. 5.15. To facilitate the comparison, some of the results with the previous settings/changes in the model are repeated in the same figure. Clearly, the comparison with observations of incident short wave radiation at the surface improves even more with this last modification.
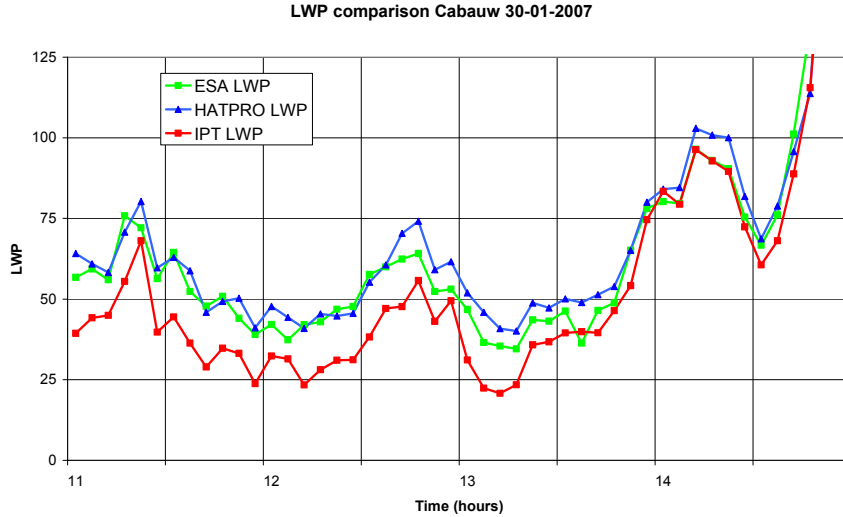
● ● ● ● 16 Evaluation of specific CCN parameterizations in the framework of the RACMO2 radiation module

LWP comparison Cabauw 30-01-2007

Figure 5.14 - The LWC time series from the IPT aggregated every 5 minutes compared to LWP from other methods
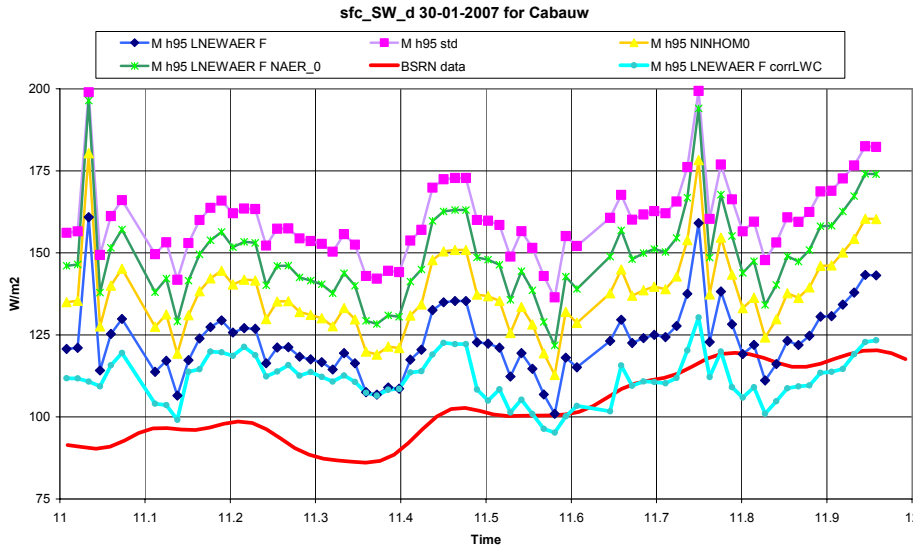
sfc_SW_d 30-01-2007 for Cabauw

Figure 5.15 - Light blue curve: Incoming SW at surface with corrected LWC input.

5.5 Improving the comparison with TOA data through changes in the model settings and the input

To improve the comparison between model and observations at the TOA the modifications discussed in the previous paragraphs have been examined in their effects on the SW radiation going out at TOA. The graphs in the figure 5.16 illustrate the comparisons between the data (in red) and different configurations of the model. Here again only the time interval between 11 and 12 UTC has been considered, when the comparison was originally the worst. Switching off the inhomogeneity factor that reduces LWC to 70% of the input value in the default configuration, improves the comparison at the TOA (compare the purple and the brown curves respectively), similarly to what is found at the surface. An even better comparison can be achieved by switching off

the new aerosol scheme (light blue curve in the Fig. 5.16). None of the other experiments is found to perform better than this last case. The experiment that gave the best comparisons between model and observations at the surface, that is the one with enhanced LWC input values, gives an amount of SW leaving at the TOA lower than found with the original LWC values.

The plots of figure 5.17 show the differences between model and observations at TOA as it was for the standard setting (left panel, between 7 and 17 UTC) and with the new aerosol scheme off, and the whole amount of LWC taken in consideration (right panel, only between 11 and 12 UTC). In summary, the differences for the SW going out at TOA, more than 110 W/m2 in the original set-up, can be reduced to ~ 40 W/m2, meaning that a considerable improvement has been achieved, but a gap between model and observations remains that can not be explained yet.
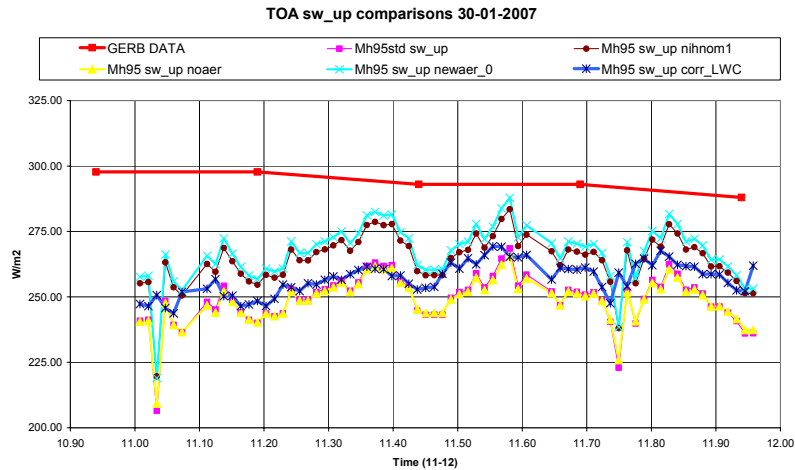
● ● ● ●   17   Evaluation of specific CCN parameterizations in the framework of the RACMO2
radiation module

Figure 5.16 - SW going up at TOA: Comparison of model output and data for different numerical experiments
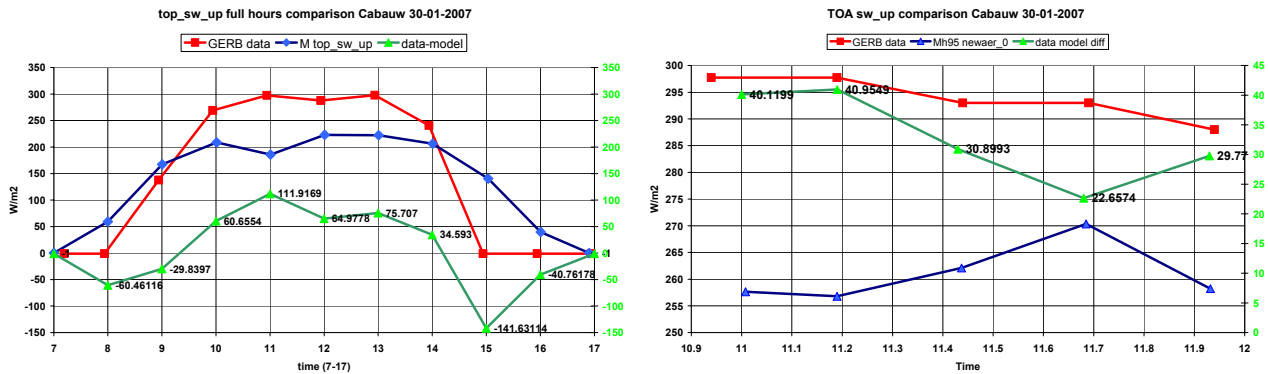

Figure 5.17 - SW going up at TOA: Differences model output and data for different tests

5.6 Summary and conclusions

Table 1 gives an overview of the different experiments that have been performed in order to test the new CCN parameterization schemes. The "AVE 40" tests have been performed using a high K factor (the effective radius is almost the same as the volume radius) of .95, in combination with the inhomogeneous mixing scheme. An hourly average value of the IPT data and the daily averaged aerosol data have been used as input. The model kept the 'standard' settings, that is the inhomogeneity factor remained set at 0.7 (NINHOM at 0.7, only 70% of available LWC is actually used in the radiation scheme); moreover the new aerosol climatology (NEWAER in the model) was used. All four CCN parameterizations have been tested. Differences between the four modeled surface and TOA SW radiations values on one hand and the measured values on the other end are found much larger than the differences among the four CCN parameterizations. This outcome makes it very difficult to decide on the basis of performances which of the CCN parameterizations is the most appropriate for use in RACMO2.

Many sensitivity tests have been conducted to assess the origin of this large discrepancy. Successive experiments

(VAR 40 and 60) have been carried out using aerosol fields interpolated on the times of the IPT data, using the model with 40 or 60 vertical levels (the top being the same, the only change is in the resolution of the layers). In these cases the effect of the K factor and of the mixing scheme has been investigated and the results are again compared with surface and TOA data. Results show that a considerable improvement can been obtained when using the Menon CCN parameterization in combination with a high K factor and the homogeneous mixing scheme (this test has been called STD60). The vertical resolution does not play a role. To further improve the comparisons a few switches have been turned off in the model, namely the NINHOM (all the available LWC used in the radiation computations) and the NEWAER (an older aerosol database is used for the direct aerosol effect computation). These two final changes produce the best comparison with the data at TOA (test Newaero, in blue in Table 1). To achieve an even better comparison at the surface, the LWC inferred from the IPT data has been enhanced, following the outcome from a standard statistical retrieved method applied to the radiometer measurements (test LWCcorr, green line in Table 1).

● ● ● ●   18   Evaluation of specific CCN parameterizations in the framework of the RACMO2
radiation module

The overall conclusion is that the degree of freedom of the model is so wide that it will anyway overshadow the differences that arise from the use of different CCN parameterizations. Given the tiny layer of cloud of this specific day, it is possible to justify the use of the homogeneous mixing scheme (effective radius not

function of the height); The choice of a high factor (0.95) to transform volume radius into effective radius could be explained by the presence during at least the first half of the testing day of 'clean' air coming from the see, but all the other settings (switching on/off schemes) do not have a solid theoretical explanation.

Exp #L	CCN par	K	mix-scheme	Aerosol input / IPT	NINHOM	NEWAER
AVE 40	BL, L, M, R	.95	inhomogeneous	At each hour	0.70	Yes
VAR 40	BL, L, M, R	.95/.67	Inhomog/homog	Interp @ IPT T/ ipt	0.70	Yes
VAR 60	BL, M	.95/.67	Inhomog/homog	Interp @ IPT T/ ipt	0.70	Yes
STD 60	M	.95	homogeneous	Interp @ IPT T /ipt	0.70	Yes
Ninhomo	M	.95	homogeneous	Interp @ IPT T/ ipt	1	Yes
Newaero	M	.95	homogeneous	Interp @ IPT T/ ipt	1	No
LWCcorr	M	.95	homogeneous	Interp @ IPT T/ LWC	1	No

Table 1 - *Summary of tests. In green the option performing best for the comparison with BSRN data, in blue the same for the GERB data.*

6 Bibliographic review of articles related to the parameterization of precipitation (autoconversion schemes) for use in (regional) climate models

The RACMO2 model uses the same autoconversion scheme of the European centre (IFS model cycle 31), that is the Sundqvist, (1978) scheme. This is a model for non-convective condensation processes that allows condensation to begin before relative humidity reaches 100%. In this scheme, the rate of condensation is a function of the relative humidity and moisture flux convergence, and the rate of precipitation formation is a function of the amount of cloud water. The scheme also takes into consideration the evaporation from falling water. The precipitation is parameterized as

$$P = C_o m[1 - exp\{-(m/m_r)^2\}] = C_m m$$

In the formula, the C's have the dimension of time^{-1}, and this means that C_m^{-1} is the typical time of conversion of droplets into raindrops. Small values of the ratio m/m_r give a conversion time that is comparatively long, with a non-precipitating cloud. As m/m_r becomes closer to 1, the conversion time becomes shorter, and the cloud becomes an efficient precipitator. The parameter m_r is a representative value of the water content at which a cloud typically comes into a well-developed precipitating state. Instead of mixing ratios m and m_r, the parameterization makes use of the concentrations of liquid water. In the original formulation $m_r = 0.5 \times 10^{-3}$ (0.5 gm^{-3} at 800-850 hPa), while $C_o = 10^{-4}$ s^{-1} (that is a conversion time of 2.8 hours). Tables are given for the values of C_m^{-1} as function of m.

The article by Rotstayn, (1997) gives a good overview of the precipitation schemes that are applied in large-scale models, at least up to the late 90's. In the same article a

new scheme is introduced, to be used in the CSIRO (Commonwealth Scientific and Industrial Research Organization, Australia) atmospheric general circulation model. His parameterization includes the liquid water cloud fraction (C), the dynamic viscosity of the air (μ), the density of water and air (ρ_w and ρ), the mean collection efficiency (E_{AU}), the droplet concentration (N_d), the acceleration of gravity (g), and the Heaviside unit step function (H), which suppresses autoconversion until the ratio q/C reaches a critical value q_{CR}.
The parameterization by Rotstayn is:

$$(q_l)_{AU} = -C_l \frac{0.104 g E_{AU} \rho^{4/3}}{\mu (N_d \rho_w)^{1/3}} \left(\frac{q_l}{C_l}\right)^{7/3} H\left(\frac{q_l}{C_l} - q_{CR}\right),$$

in which the critical mixing ratio q_{CR} is given by:

$$q_{CR} = \frac{4}{3} \pi \rho_w r_{CR}^3 N_d / \rho$$

Here, r_{CR} is the critical mean droplet radius at which autoconversion begins. E_{AU}, r_{CR} and N_d are given.

A more recent article by Penner et al., (2006), on a model intercomparison of indirect aerosol effects, describes the autoconversion schemes used in three state-of-the-art GCMs, that is the French Laboratoire de Météorologie Dynamique- Zoom (LMD-Z) model, the Japanese Center for Climate System Research (CCSR) model and the NCAR Community Atmosphere Model (CAM 2.0.1), modified at the University of Oslo. The LMD model uses an autoconversion scheme derived by Chen and Cotton, (1987), ignoring the term that involves spatial inhomogeneities in liquid water. The CAM model uses again the scheme by Chen and Cotton (1987), with

modification by Liuo and Ou, (1989), while the CCSR model uses the scheme by Berry, (1967). All these schemes include explicitly the droplet number concentration, N_d. In the article, for a comparison, all the models are run once with a common autoconversion parameterization, that is the one by Khairoutdinov and Kogan, (2000), that only includes liquid water mixing ratio and droplet number concentration:

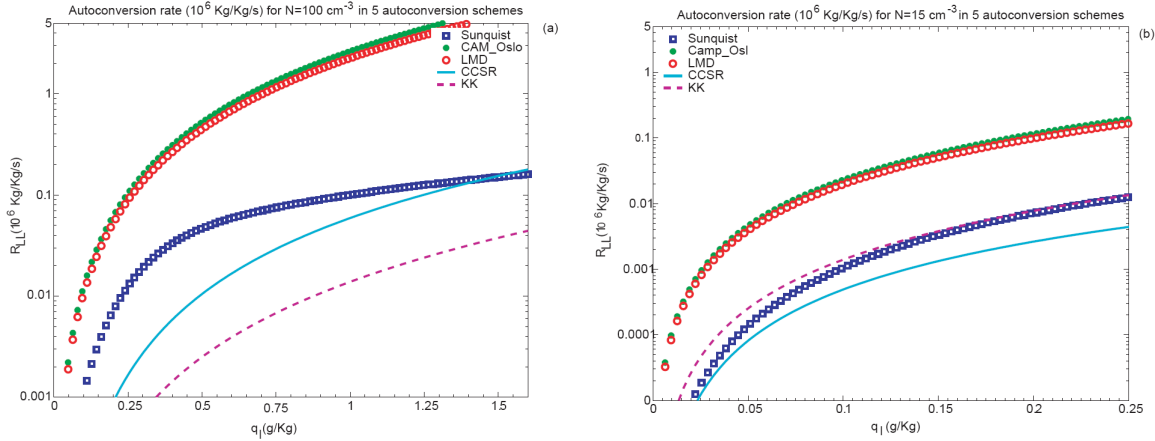$$P = 1350 q_l^{2.47} N_d^{-1.79}$$

The curves of figure 6.1, from the article by Penner et al., (2006) shows the autoconversion rates as a function of liquid water mixing ratio for different types of schemes, and for two values of droplet concentration, that is 100 cm⁻³ (panel a, left) and 15 cm⁻³ (panel b, right).
The curves show that, for very low values of N_d, there is no great difference among the Khairoutdinov and Kogan (2000), the Sundqvist, (1978) and the Berry, (1967) schemes; the two different modifications of the Chen and Cotton, (1987) scheme, used in the CAM_Oslo and LMD models, give a very similar autoconversion rate. This is true also with a larger N_d amount, while the first three schemes present large differences among them.

Figure 6.1 - *Autoconversion schemes comparison (after Penner et al., (2006))*

7   Conclusions and remarks

A working version of the SCM of the RACMO2 model including a new set of CCN parameterizations and new schemes for the calculation of the effective radius for the computation of the SW radiation has been developed. Evaluation studies have been performed for a single day (in the available dataset) on which a single water cloud layer was present above Cabauw, and IPT and MARGA data were available all together for the same location. From these tests it is evident that model specific parameters, which cannot be constrained by observations, play a very important role, but also an apparent systematic bias in the LWP estimated from IPT for low LWP is found to have a considerable effect on the outcome. Nevertheless, it is possible to achieve a reasonably good comparison with data.

Though the tests we performed are inconclusive, since they are not significant in a statistical sense, we suggest using the Menon et al. (2002) parameterization. This parameterization, still simple to implement, has more than one aerosol type already, and might be extended to include also nitrate; moreover it gave the best comparison against data, in the evaluation. It should be noticed that the aim of this part of the project is to model the cloud albedo in both the present as in the pre-industrial time, and to be able to produce scenarios for the future. To this scope, the newly implemented modules in the SCM appear to be a sufficiently good solution. In the near future, the 3D version of RACMO2 will be updated, including these new modules.

Appendix 1 - Parameterization of CCN and related matters in RACMO2

The SCM (single column model) version of RACMO2 (using the ECMWF model physics package) has been installed on a workstation and a standard simulation run has been successfully completed as preliminary test. The structure of the code has been analyzed to understand the way radiation (short wave component) is computed and used throughout the model. Originally, the SCM (cycle 31) had the possibility to compute the effective radius for liquid water particles in three different ways (see file `radlsw.F90` for the code). In the first case, an empirical parameterization is used to compute the mean effective radius, as a linear function of the height, from 10 μm at the surface to 45 μm at the top of the atmosphere (code incorrect!).

The second approach just prescribes two fixed values of effective radius, utilized for the complete column, one of 10 μm for land points, and one of 13 μm for sea points. This option is set as standard configuration of the SCM. The third option is to use the formula by Martin et al., (1994) to obtain the effective radius. For the Bsik KvR CS4-project a fourth way to calculate the effective radius for liquid water particles has been introduced in the SCM radiation code. To use this new option, the column of interest has to be extracted from the netCDF files with the LOTOS-EUROS aerosol fields and written to a new netCDF forcing file.

During a model run, the required aerosol concentrations (SO4 and fine sea salt) and LOTOS level heights are read from the forcing files every model hour and the aerosol concentrations are vertically interpolated to the model levels. At intermediate time steps the concentrations are linearly interpolated. Both reading the forcing files and

the interpolations are carried out by the `getlotos` subroutine. At every model time step the aerosol concentrations are translated to the concentration CCN in the `ndlotos` routine using one of four parameterizations (the choice and the properties of these parameterizations have already been discussed in this report): Boucher and Lohmann, Lowenthal et al., Menon et al., or Rotstayn. So far, it has been assumed that all CCN becomes activated so that the droplet concentration is equal to the concentration of CCN. For all levels with cloud, the droplet concentration at cloud base is converted to the effective radius in the routine `refflotos`. The effective radius is calculated using either the inhomogeneous (the effective radius is a function of height from cloud base) or the homogeneous mixing model (the droplet concentration is constant with height, the effective radius is a function of the liquid water content) (see appendix A in the article by Boers et al., (2006) for a formal description of these two schemes). If the cloud extends above the LOTOS limit of 3500m (or 5000m), a fixed effective radius of 10 micron over land and 13 micron over sea is assigned to the model levels above these limits. The effective radius calculated by `refflotos` is used in the radiation scheme of the model as it was before. The user can set the CCN parameterization and the mixing model to be used by the SCM through a newly introduced namelist, `naelotos` inside the `fort.4` file. Additionally, several other variables, such as the conversion factor from droplet radius to effective radius and the location of the aerosol forcing files can be set using this namelist.

Acknowledgements

Bibliography

Abdul-Razzak, H. and Ghan, S., (2002), A parameterization of aerosol activation. 3. Sectional representation, *JGR*, vol. 107, NO. D3.

Abdul-Razzak, H. and Ghan, S., (2004), Parameterization of the influence of organic surfactants on aerosol activation, *Journal of Geophysical Research*, 109(D3): doi: 10.1029/2003JD004043.

Abdul-Razzak, H., S. Ghan and C. Rivera-Carpio, (1998), A parameterization of aerosol activation 1. Single aerosol type, *J. Geophys. Res.*, 103, 6123-6131.

Berry, E. X., (1967), Cloud droplet growth by collection, *J. Atmos. Sci.*, 24, pp. 688–701.

Boers, R., J.R. Acarreta, and J.L. Gras, (2006), Satellite monitoring of the first indirect aerosol effect: Retrieval of the droplet concentration of water clouds, *Journal of Geophysical Research*, vol. 111, D22208.

Boucher, O. and H. Rodhe, (1994), The sulfate-CCN-cloud albedo effect: A sensitivity study, *Report CM-83*, Department of Meteorology, Stockholm University, 20 pp.

Boucher, O. and U. Lohmann, (1995), The sulfate-CCN-cloud albedo effect, A sensitivity study with two general circulation models, *Tellus*, 47B, pp. 281-300.

Charlson, R. J., J. H. Seinfeld, A. Nenes, M. Kulmala, A. Laaksonen and M. C. Facchini, (2001), Reshaping the Theory of Cloud Formation, *Science*, vol. 292, pages 2025-2026.

Chen, C. and Cotton, W. R., (1987), The physics of the marine stratocumulus-caped mixed layer, *J. Atmos. Sci.*, 44, pp. 2951–2977.

Chuang, C.C. and J.E. Penner, (1995), Effects of anthropogenic sulphate on cloud drop nucleation and optical properties, *Tellus*, 47, 566-577.

Coakley, J. A., Jr., and P. Chýlek (1975), The two stream approximation in radiative transfer: Including the angle of the incident radiation, *J. Atmos. Sci.*, 32, 409-418.

De Martino, G., R. Boers, M. Schaap and H.M. ten Brink, (2006), Comparative study of cloud droplet number concentration parameterizations for use in regional climate models, Poster: EGU general Assembly, 2/4/2006-7/4/2006, Vienna, Austria, European Geophysical Union.

de Roode, S.R., A. Los, (2008), The effect of temperature and humidity fluctuations on the liquid water path of non-precipitating closed-cell stratocumulus clouds, *The Quarterly Journal of the Royal Meteorological Society*, Volume 134 Issue 631, p. 403 - 416.

Elbert, W., M. R. Hoffmann, M. Krämer, G. Schmitt and M. O. Andreae, (2000), Control of solute concentrations in cloud and fog water by liquid water content, *Atmos. Environ.*, 34, p. 1109-1122.

Feingold, G., B. Stevens, W. R. Cotton, and A. S. Frisch, (1996), The relationship between drop in-cloud residence time and drizzle production in numerically simulated stratocumulus clouds, *J. Atmos. Sci.*, 53, 1108-1122.

Fuzzi et al., (1992), The Po Valley Fog Experiment 1989. An Overview, *Tellus*, 44B, pages 448-468.

Fuzzi et al., (1994), Multiphase Chemistry and Acidity of Clouds at Kleiner Feldberg, *J. Atm. Chem*, 19, pages 87-106.

Fuzzi, M. Gysel, A. Laaksonen, U. Lohmann, T. F. Mentel, D. M. Murphy, C. D. O'Dowd, J. R. Snider, and E. Weingartner, (2005), The effect of physical and chemical aerosol properties on warm cloud droplet activation, Atmos. Chem. Phys. Discuss., 5, 8507–8646.

Ghan, S.J., C. Chuang and J.E. Penner, (1993), A parameterization of cloud droplet nucleation part I: single aerosol type, *Atmos. Res.*, 30, 197-211.

Glantz, P. and K.J. Noone, (2000), A physically-based algorithm for estimating the relationship between aerosol mass to cloud droplet number, *Tellus*, 52, 1216-1231.

Gondwe, M.P., (2004), Quantifying the Role of Marine Phytoplankton (DMS) in the Present Day Climate System, Ph. D. thesis, University of Groningen.

Hegg, D.A., (1994), Cloud condensation nucleus-sulphate mass relationship and cloud albedo, *J. Geophys. Res.*, 99, 25,903-25,907.

IPCC, (2001), *Climate Change 2001, the Scientific Basis*, 3rd report.

Jones, A. and A. Slingo, (1996), Predicting cloud-droplet effective radius and indirect sulphate aerosol forcing using a general circulation model, *Quart. J. R. Met. Soc.*, 122, 1573-1595.

Jones, A., D.L. Roberts, and A. Slingo (1994), A climate model study of the indirect radiative forcing by anthropogenic sulphate aerosols, *Nature*, 370, 450-453.

Khairoutdinov, M. and Kogan, Y., (2000), A new cloud physics parameterization in a large eddy simulation model of marine stratocumulus, *Mon. Wea. Rev.*, 128, pp. 229–243.

King, M.D., Harshvardhan, (1986), Comparative Accuracy of Selected Multiple Scattering Approximations, *Journal of the Atmospheric Sciences*, Vol. 43, No. 8, pages 784-801.

Kulmala, M., A. Laaksonen, P. Korhonen, T. Vesala, and T. Ahonen, (1993), The effect of Atmospheric Nitric Acid Vapor on Cloud Condensation Nucleus Activation, *Journal of Geophysical Research*, vol. 98, No. D12, pages 22949-22958.

Laaksonen, A., P. Korhonen, M. Kulmala, and R. J. Charlson, (1998), Modification of the Köhler Equation to Include Soluble Trace Gases and Slightly Soluble Substances, *Journal of the Atmospheric Sciences*, vol. 55, pages 853-862.

Liou, K.-N. and Ou, S.-C., (1989), The role of cloud microphysical processes in climate: An assessment from a one-dimensional perspective, *J. Geophys. Res.*, pp. 94, 8599–8606.

Lohmann U. and Feichter J. (2005), Global indirect aerosol effects: a review, *Atmospheric Chemistry and Physics*, vol. 5, pp.715-737.

Löhnert, U. , S. Crewell, C. Simmer, (2004), An integrated approach towards retrieving physically consistent profiles of temperature, humidity, and cloud liquid water, *Journal of Applied Meteorology*, Vol. 43, No. 9, pp. 1295-1307.

Lowenthal, D. H., R. D. Borys, T. W. Choularton, K. N. Bower, M. J. Flynn and M. W. Gallagher, (2004), Parameterization of the cloud droplet-sulfate relationship, *Atmospheric Environment*, vol. 38, pp. 287-292.

Martin, G.M., D.W. Johnson, and A. Spice, (1994), The measurement and parameterization of effective radius of droplets in warm stratocumulus clouds, *J. Atmos. Sci.*, 51, 1823-1842.

McFiggans, G., P. Artaxo, U. Baltensperger, H. Coe, M. C. Facchini, G. Feingold, S.

Menon, S., A. D. Del Genio, D. Koch and G. Tselioudis, (2002), GCM Simulations of the Aerosol Indirect Effect: Sensitivity to Cloud Parameterization and Aerosol Burden, *J. of Atm. Science*, pp. 692-713.

MGA, (2002), *Meteorological & Geoastrophysical Abstracts*, CSA, 7200 Wisconsin Avenue, Bethesda, MD 20814 USA, CD.

Ming, Y., V. Ramaswamy, L. J. Donner, and V. T. J. Phillips, (2005), A New Parameterization of Cloud Droplet Activation Applicable to General Circulation Models, *JAS*, 63(4), 1348-1356.

Nenes, A. and Seinfeld, J.H., (2003), Parameterization of cloud droplet formation in global climate models, *J.Geoph.Res.*, 108, 4415, doi: 10.1029/2002JD002911.

Novakov, T., D.A. Hegg and P.V. Hobbs, (1997), Airborne measurements of carbonaceous aerosols on the East Coast of the United States, *J. Geophys. Res. Atmos.*, 102, 30023-30030.

O'Dowd, C.D., J. Lowe, M.H. Smith and A.D. Kaye, (1999), The relative importance of sea-salt and nss-sulphate aerosol to the marine CCN population: An improved multi-component aerosol-droplet parameterization, *Q. J. Roy. Met. Soc.*, 125, 1295-1313.

Penner, J. E., Xiquan Dong and Yang Chen, (2004), 'Observational evidence of a change in radiative forcing due to the indirect aerosol effect', *Nature*, vol. 427, pages 231-234.

Penner, J.E., J. Quaas, T. Storelvmo, T. Takemura, O. Bucher, H. Guo, A. Kirkevag, J.E. Kristjansson, (2006), Model intercomparison of indirect aerosol effects, *Atmos. Chem Phys*, 6, pp. 3391-3405.

Raga, G.B., and P.R. Jonas, (1993), On the link between cloud-top radiative properties and subcloud aerosol concentrations, *Q. J. Roy. Meteorol. Soc.*, 119, 1419-1425.

Rotstayn, L. D., (1997), A physically based scheme for the treatment of stratiform clouds and precipitation in large-scale models. I: Description and evaluation of the microphysical processes, *Quart. J. R. Met. Soc.*, 123, pp. 1227-1282.

Rotstayn, L. D., (1999), Indirect forcing by anthropogenic aerosol: A global climate model calculation of the effective-radius and cloud-lifetime effects, *Journal of Geophysical Research*, vol. 104, no. D8. pp. 9369-9380.

Schaap, M., M. Roemer, F. Sauter, G. Boersen, R. Timmermans, P.J.H. Builties, (2005), LOTOS-EUROS: Documentation, TNO-report, B&O-A R 2005/297.

Sundqvist, H., (1978), A parameterization scheme for non-convective condensation including prediction of cloud water content, *Quart. J. R. Met. Soc.*, 104, pp. 677-690.

Suzuki, K., T. Nakajima, A. Numaguti, T. Takemura, K. Kawamoto, A. Higurashi, (2004), A Study of the Aerosol Effect on a Cloud Field with Simultaneous Use of GCM Modeling and Satellite observation, *JAS*, vol. 161, pages 179-194.

Tang, I. N., (1997), Thermodynamic and optical properties of mixed-salt aerosols of atmospheric importance, *JGR*, vol. 102, No. D2, pages 1883-1893.

ten Brink, H. M., R. Otjes, P. Jongejan, G. Kos, (2007a), On the importance of nitrate as IAE-agent in western Europe, *Proc 2007 AGU fall-meeting*, San Francisco, Dec 2007.

ten Brink, H.M., R. Otjes, P. Jongejan, (2007b), On the ratio of nitrate to sulphate in CCN in the Netherlands, Proc. edited by the *American Association for Aerosol Research* (AAAR), pp 1343-1344, Available on the Bsik-KvR site

Twomey, S., (1959), The nuclei of natural cloud formation. Part II: The supersaturation in natural clouds and the variation of cloud droplet concentration, *Geophys. Pure Appl.*, 43, 243–249